INTERANNUAL AND SEASONAL VARIATIONS IN MARINE BOUNDARY LAYER CLOUD FRACTION AND LOWER TROPOSPHERIC STATIC STABILITY USING SATELLITE OBSERVATIONS AND GLOBAL CLIMATE MODEL OUTPUT

by

Kathryn W. Mozer

A thesis submitted in partial fulfillment of

the requirements for the degree of

Master of Science

(Atmospheric and Oceanic Sciences)

at the

UNIVERSITY OF WISCONSIN-MADISON

2010

Approved by: _____

Steven A. Ackerman, Ph.D.

Professor, Atmospheric and Oceanic Sciences

Director, CIMSS

Date: _____

Abstract

Marine boundary layer (MBL) clouds have a large effect on the global radiation budget because their albedo is much higher than the underlying ocean causing most incoming solar radiation to be reflected, while longwave radiation is emitted at the same rate as the ocean surface leading to a net cooling effect in the MBL. Thus, simulating MBL clouds in General Circulation Models (GCM) is crucial in future climate predictions, however, these clouds are poorly simulated. One technique to resolving this issue is incorporating lower tropospheric static stability (LTS) into model cloud parameterization schemes. LTS has been previously shown to correlate well with MBL clouds (particularly stratiform) on seasonal to interannual time scales. This study asks if LTS is a good proxy for predicting the observed amount and variability of MBL cloud both interannually and seasonally, and how well do climate models simulate these patterns?

An area in the eastern South Pacific is chosen for this study as it is dominated by MBL stratiform clouds year-round. The Advanced Very High Resolution Radiometer (AVHRR) Pathfinder Atmospheres Extended dataset (PATMOS-x) provides a unique opportunity to study MBL clouds over the past 28 years with fine resolution. NCEP/Reanalysis data is used to compute LTS for comparison to MBL clouds. Observational data is compared to one realization of two model experiments (Climate of the 20th Century and SRESa1b) for two separate coupled GCMs used in the 2004 Intergovernmental Panel on Climate Change (IPCC) Assessment Report: NCAR/CCSM3.0 and GFDL/CM2.0. Results show CM2 simulates MBL cloud interannual variability well from 1982-1999. However, both models poorly simulate MBL cloud seasonal variability

compared to observations. Interestingly, the relationship between MBL cloud fraction and LTS is weak in the observations in most seasons, even more so at interannual scales, and inconsistent with relationships between LTS and cloud fraction observed in models. These findings call into question previous studies suggesting a strong link between LTS and cloud fraction, at least for the study region. Potential reasons for this and ways to better parameterize MBL clouds in climate models are discussed.

Acknowledgements

I would first like to thank my advisors Steve Ackerman and Andy Heidinger for giving me the opportunity to further my education at UW-Madison. The experience has been invaluable and I feel extremely lucky to have been chosen as one of their students. I would also like to thank Ankur Desai for his insight and comments while completing this work in addition to selecting me as his teaching assistant in my final semester which proved one of the most rewarding parts of my graduate school career.

It goes without saying that my parents and sister are the reason I have reached this point. I am forever grateful for the constant encouragement, support, and understanding that my parents have given my entire life. Also, for instilling in me the drive and motivation to do anything I put my mind to. My sister deserves a big 'thank you' for being the best role model a younger sister could have and knowing that I could achieve the same great things that she achieved.

Finally, I would like to thank my office mates Mark Smalley, Brent Maddux, Erin Wagner and all of the wonderful friends I have met during this time. Without their guidance, support, and institutional knowledge I would probably not have graduated in a timely fashion. A final thank you is extended to Brian Miretzky for his support, encouragement, and ability to make me laugh.

Table of Contents

I. Introduction

a. Background

Subtropical low stratiform clouds typically form in the marine boundary layer (MBL) over the eastern regions of the world's oceans. Their reduction to the earth's radiation budget is significant and this climate sensitivity is difficult to parameterize in global climate models. Thus, MBL stratiform clouds, their microphysics, and seasonal variations, are a heavily studied topic of research (Klein and Hartmann 1993 herein referred to as KH93).

The sensitivity of tropical MBL clouds to changing environmental conditions has been identified as the leading error in global climate models (Bony and Dufresne 2005). In Bony and Dufresne (2005), the authors study cloud radiative forcing in the 15 coupled ocean-atmosphere global climate models used in the Fourth Assessment Report of the Intergovernmental Panel on Climate Change (IPCC). They conclude that the largest discrepancies in climatic change in the models occurs in large-scale subsidence regimes (representative of the tropics) and most models underestimate the interannual sensitivity of albedo to a temperature change in MBL clouds. One contributing factor to these discrepancies is that MBL clouds are formed by processes that occur on smaller scales than are resolved by global climate models (Stephens 2004) consequently requiring empirical parameterization.

Subtropical marine stratiform clouds form beneath a strong temperature inversion within the boundary layer and above a cold ocean sea surface. Moisture from the sea surface evaporates and reaches saturation within the boundary layer. Convection is maintained due to radiative cooling at the top of the clouds that form. The Hadley circulation provides

subsidence to the region allowing the temperature inversion to cap the boundary layer keeping the stratocumulus confined to it (KH93). The albedo of these clouds is larger than the ocean surface below and as a result, solar radiation is not well absorbed. Thus, there is strong radiative cooling at cloud top and weak radiative warming at cloud base (Petty 2006). The amount of emitted thermal radiation does not compensate for the absorption deficit and thus, there is a global negative feedback on the radiative forcing (Jensen et al. 2008).

KH93 discovered an empirical relationship between stratocumulus cloud fraction and atmospheric stratification in the subtropical stratiform regions: the season with the greatest amount of stratiform clouds correlates with the season with the greatest lower tropospheric static stability (LTS). LTS is a measure of inversion strength and defined as the difference in potential temperature between 700 mb and the surface. A high LTS indicates a greater difference in potential temperature between the two levels implying a strong inversion. This supports the idea that stratiform clouds are most abundant under a well-defined temperature inversion and are not necessarily sensitive to sea surface temperatures alone.

b. Motivation

The relationship between MBL stratiform clouds and LTS has been studied recently with various observation data but only for short time periods (Jensen et al. 2008, Ghate et al. 2009, Zhang et al. 2010). PATMOS-x provides a unique opportunity to study this relationship as it is a 28 year satellite dataset. Using this dataset to compare to GCM model output allows for a much more comprehensive analysis of GCM performance of MBL stratiform cloud coverages and if there is a strong relationship with LTS over time.

In order to make comparisons with previous studies, a 20°x20° box in the eastern South Pacific was chosen (5-25 S and 80-100 W, Figure 1). The box encompasses the area selected by KH93 and is slightly smaller than the box used in Jensen et al. (2008) and Zhang et al. (2010). This particular area is chosen since MBL stratiform clouds are present throughout the entire year, with June through December dominated by 60% or greater low cloud cover (KH93). Other areas of MBL stratus were found to correlate extremely well with LTS, in that the maximums and minimums of clouds corresponded to the same maximums and minimums in LTS seasonally.

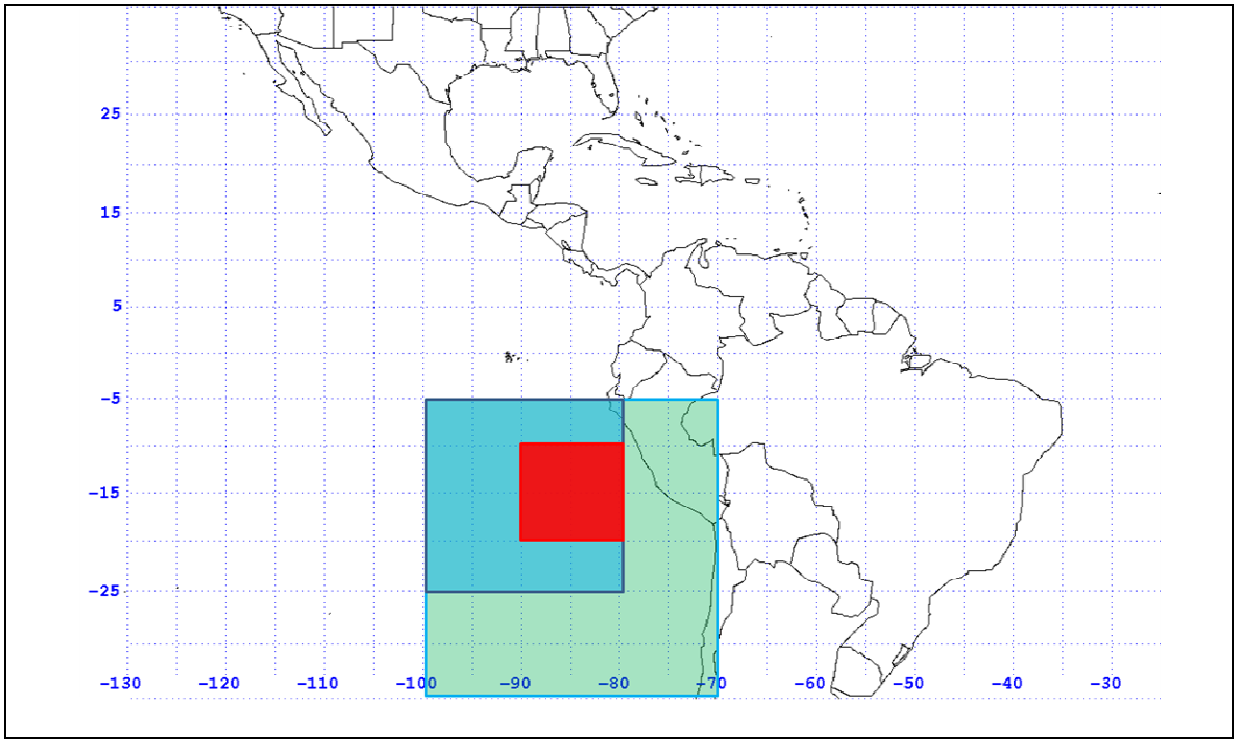

Figure 1. Area for this study (5-25 S, 80-100 W) is shown as the medium size box in bright blue. It is smaller than the box used in Jensen et al. (2008) and Zhang et al. (2010) shown in light green (5-35 S, 70-100 W) to eliminate effects of land, and it is larger than the box used in KH93 shown in red (10-20 S, 80-90 W) to capture more of the MBL region.

Figure 2 shows the low cloud fraction-LTS relationship (which is on a seasonal scale) for PATMOS-x and NCEP/Reanalysis LTS. Figure 3 is from KH93 and shows low cloud fraction for area they studied showing a similar interannual pattern as PATMOS-x.

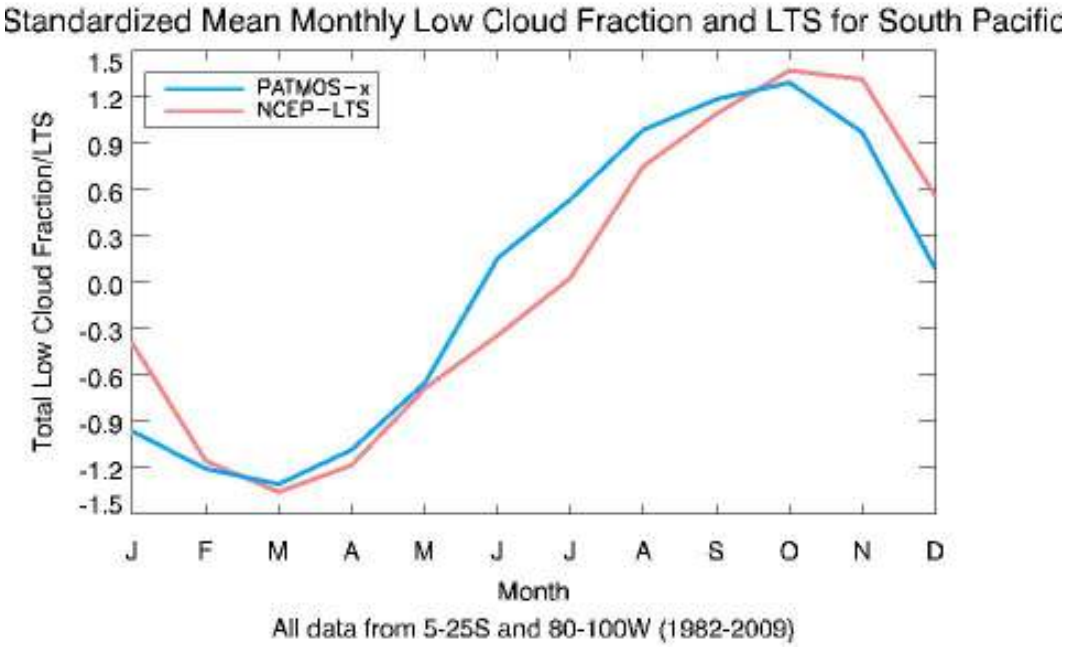

Figure 2. Seasonal cycle of observed low cloud fraction from PATMOS-x (blue) and observed LTS from NCEP/Reanalysis data (red) for years 1982-2009. Months are composed of monthly means that have been standardized by subtracting the average of all 12 months from each month value and dividing by the standard deviation.

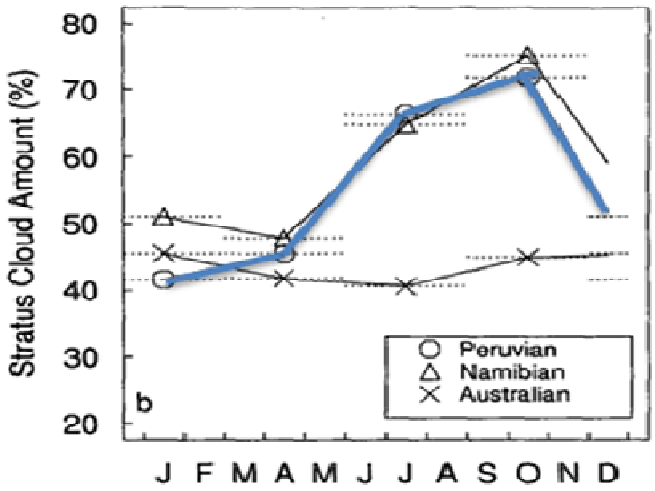

Figure 3. Seasonally averaged stratus cloud amount from KH93. The blue line highlights the Peruvian stratus region that corresponds to the region defined for this study. Data is from ship observations taken from the Comprehensive Ocean-Atmosphere Data Source (COADS) between December 1951 and November 1981.

Cloud fraction in both figures follows a similar pattern as seen in Figure 4 where Figure 3 has been superimposed onto PATMOS-x low cloud fraction. Values for PATMOS-x are lower than KH93 and possible reasons for this are presented in the discussion section. The 28 year pattern in Figure 2 appears to correlate well with low cloud fraction further supporting KH93 on a much larger time scale than other recent studies.

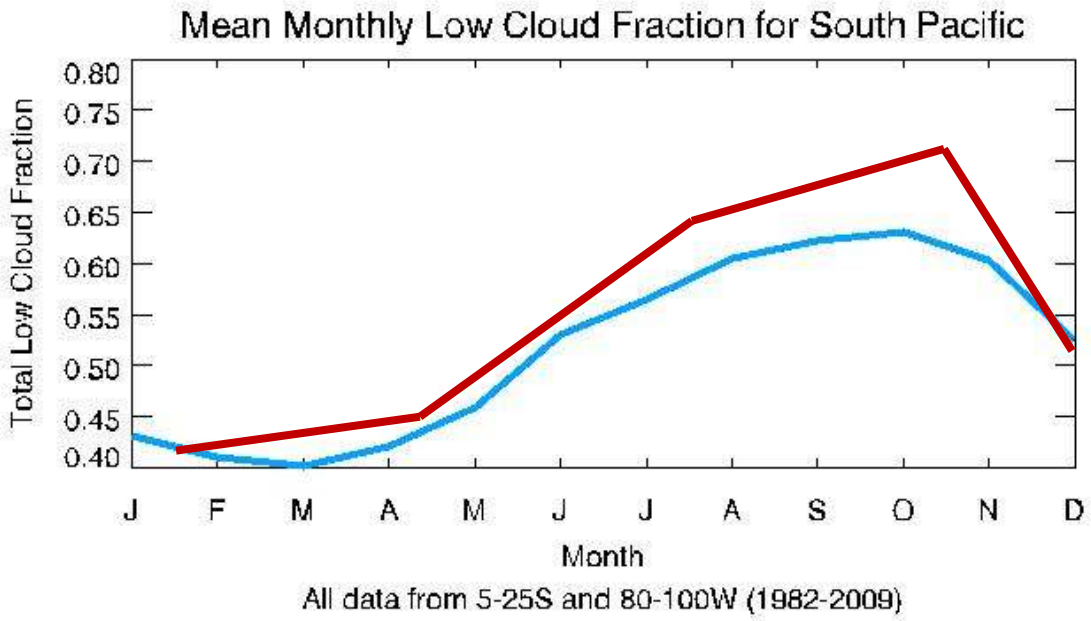

Figure 4. Blue line is PATMOS-x monthly mean low cloud fraction from 1982-2009. Red line is seasonally averaged low cloud fraction from KH93 for 1951-1981.

c. Thesis Objective

The purpose of this study is to determine how well global climate models predict low cloud fraction with respect to LTS in the well known stratus dominated area in the eastern South Pacific by comparing various GCM experiments to the PATMOS-x satellite dataset from 1982-2009. Given the vast amount of GCM output available, only one run from two separate experiments for two different models is used to calculate their respective low cloud fraction and LTS. NCEP/Reanalysis data is used to calculate observation LTS. Section II will discuss the specifics of all the data used. The results of the study are presented in section III.

Sections IV and V will strive to analyze the results as well as answer the following questions driving the study:

-Is there a relationship between PATMOS-x low cloud fraction and NCEP-LTS that supports the initial empirical relationship first presented by KH93?

-Do models accurately represent low cloud fraction at interannual and seasonal scales?

-Do models show the same relationship between low cloud fraction and LTS as observations both seasonally and interannually?

-Does the NCAR/CCSM3 model simulate low cloud fraction more accurately than the GFDL/CM2 model since it incorporates LTS into its cloud parameterization scheme for low clouds?

II. Datasets

a. PATMOS-x data set

1. Description

The data set used in this study is the latest version of the Advanced Very High Resolution Radiometer (AVHRR) Pathfinder Atmospheres Extended dataset (PATMOS-x). It is an extension of the original PATMOS data set that includes additional algorithms, products, and temporal coverage (Heidinger and Pavolonis 2009). The dataset is comprised of reprocessed AVHRR data from the Polar Orbiting Environmental Satellites (POES) from 1981 to the present (CIMSS-A). The AVHRR is a 5 channel imager with a nominal spatial resolution of 1.1 km. The Global Area Coverage (GAC) used in this study has an effective spatial resolution of 4 km. PATMOS-x currently uses data from the AVHRR/2 and AVHRR/3 (NOAASIS). The PATMOS-x data consist of sampled GAC Level-2 results mapped to a 0.1° equal-angle global grid. This PATMOS-x data format is referred to as Level-2b. It is important to note that each point in the Level-2b data represents information from one pixel without any spatial or temporal averaging. This was done to preserve the non-linear relationships among the various cloud properties (personal correspondence, Andrew K. Heidinger 2010). The Level-2b data is computed for each satellite, for each day, and for both ascending and descending nodes (twice daily) (CIMSS-B). Data spanning the time range from January 1, 1982 through December 31, 2009 are used to compare with GCM output. There are approximately 40,000 data points in this study domain.

2. Satellite Drift

The satellites used in the PATMOS-x dataset are NOAA-7, 9, 11, 12, 14, 15, 16, and 18. Their local equator-crossing time (ECT) ranges from 0130 to 0230 for the descending

node and 1330 to 1430 for the ascending node. Over time, the orbits of these satellites drift so that their ECT becomes later as illustrated in Figure 5 (Gutman 1999). To compensate for this issue, a third degree polynomial is calculated to fit the data being used given a specific local observation time, in this case 1400. The difference between each point's value on the fit line and the value at 1400 is calculated and added back to the original value of each point. This essentially calculates and adjusts the data to a diurnal pattern.

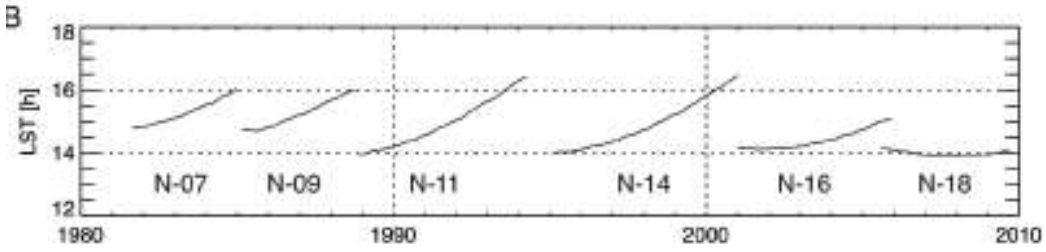

Figure 5. Local ascending observation time for most satellites used in this study adapted from Rausch et al. (submitted August 2010).

3. Cloud Algorithms

In order to compare low cloud fraction to GCM low cloud fraction effectively, an understanding of the cloud fraction algorithm is essential. First, each pixel is determined as cloudy or clear by a Bayesian cloud algorithm (personal correspondence, Andrew K. Heidinger 2010). Then the cloud typing algorithm for PATMOS-x is used which is partly described here (a more detailed explanation can be found in Pavolonis et al. 2005). Cloudy pixels from AVHRR, during daytime, are classified by two separate algorithms into several cloud types: warm liquid water clouds, supercooled-mixed-phase clouds, opaque ice clouds/deep convection, nonopaque high ice clouds, and cloud overlap. Satellites previous to

NOAA-14 only have 5 channels (bands 0.63, 0.86, 1.6, 10.8, and 12.0 μm) while satellites flown after NOAA-14 have 6 channels (bands 0.63, 0.86, 1.6, 3.75, 10.8, and 12.0 μm). This is the reason for two separate algorithms; more recent satellites can switch between channels 3a (1.6 μm) and 3b (3.75 μm) (Pavolonis et al. 2005).

The AVHRR algorithm decision tree is shown in Figure 6. Each pixel must pass one of four tests based on the brightness temperature at 11 μm (BT(11)) after which it goes through a cloud overlap test (Pavolonis et al. 2005). Pavolonis and Heidinger 2004 state that cloud overlap refers to multilayered cloud systems which can be challenging to detect from a satellite as a high cloud layer can mask a lower cloud layer from being sensed, or a high cloud layer might be too thin for detection if a thicker, lower cloud layer is present. A split-window approach is used in the cloud overlap algorithm for AVHRR as well as the 0.65 μm reflectance for a single cloud layer. This approach uses the difference in 11 μm and 12 μm brightness temperatures as a way to determine cirrus cloud. Figure 6 shows the test a pixel goes through to determine if overlap may be present. One constraint of the test is if the split-window brightness temperature difference is greater than a given threshold for a 0.65 μm reflectance. Also, the 0.65 μm reflectance must be at least 30% in order to prevent thin cirrus over a bright surface at 0.65 μm (such as a desert) from being classified as cloud overlap. A further constraint to the algorithm is the BT(11) must be less than 270 K. This is because a layer of broken water clouds or the edge of a water cloud can have a reflectance greater than 30% and a large brightness temperature difference which would incorrectly classify it as cloud overlap. However, these clouds also tend to have a BT(11) greater than 270 K, which is why the constraint is set to less than 270 K. Problems with this constraint include the

tendency for high, thin cirrus over low, water cloud to be missed as well as thin cirrus over a snow or ice surface to be misclassified as cloud overlap (Pavolonis and Heidinger, 2004).

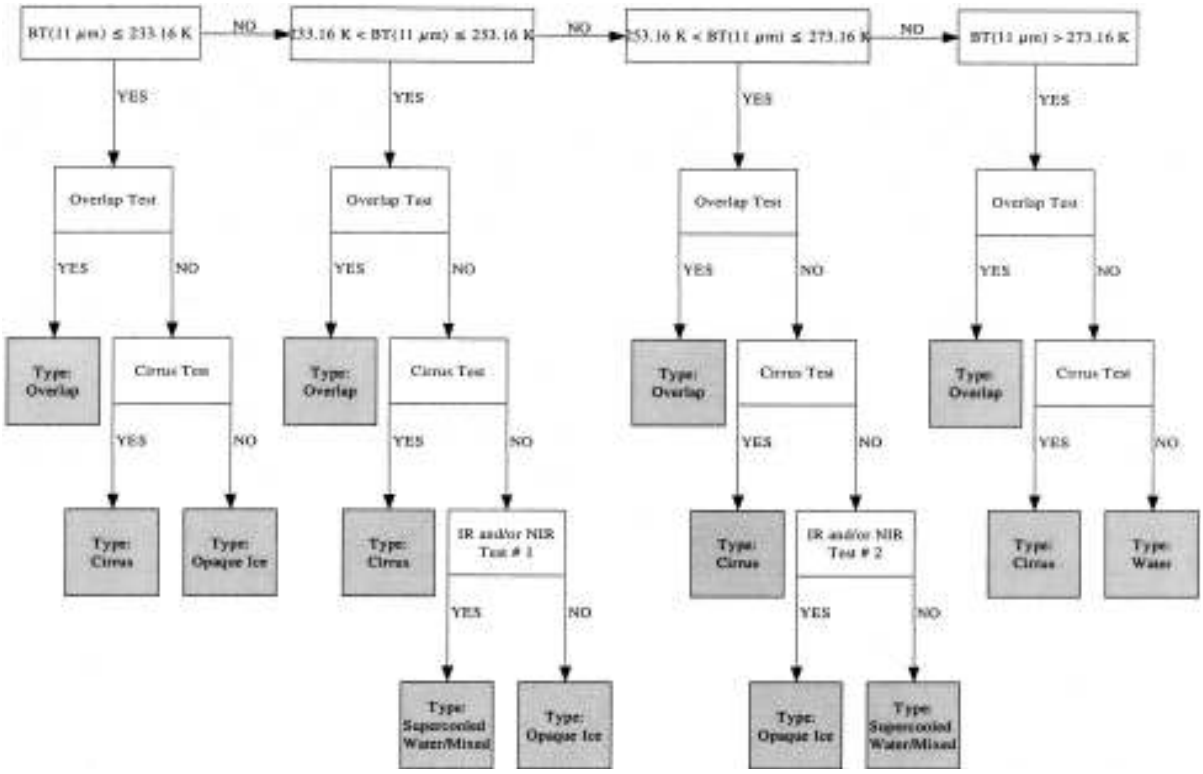

Figure 6. AVHRR cloud-typing algorithm decision tree from Pavolonis et al. (2005).

If the cloud overlap test succeeds, the pixel is classified as a multi-layered cloud condition. If it fails, there are several more tests a pixel will endure until the proper cloud classification is reached which are described here from Pavolonis et al. 2005. A pixel is tested for nonopaque ice clouds with the AVHRR cirrus detection test if BT(11) < 233.16 K. The pixel is considered either opaque ice cloud if the cirrus test fails, or nonopaque ice cloud if the test succeeds. The cirrus test is also performed if 233.16 K < BT(11) ≤ 253.16 K. If it

fails, the near-infrared (NIR) reflectance test 1 is used. NIR reflectances are used to infer cloud phase based on reflectance thresholds that are determined from 1.65 μm and 3.75 μm bands (channels 3a and 3b) depending on which is used. Table 1 lists the reflectance thresholds.

Table 1. NIR thresholds from Pavolonis et al. (2005).

Surface type	NIR threshold (1.65 μm)	NIR threshold (3.75 μm)
water/snow/ice	0.25 (25%)	0.06 (6%)

A supercooled water/mixed-phase cloud is determined if a pixel has a NIR reflectance greater than the threshold value. If the NIR reflectance value is less than the threshold, the pixel is considered opaque ice cloud type. For 253.16 K < BT(11) ≤ 273.16 K, the cirrus test is also performed. If the pixel values fail the cirrus test, the NIR reflectance test 2 is used. In this version, the pixel is considered opaque ice cloud if the NIR reflectance is less than the threshold value and BT(11) < 263.16 K. If those conditions are not satisfied, the pixel is classified as supercooled water/mixed-phase cloud type. Finally, the cirrus test is used if BT(11) > 273.16 K. The pixel is considered nonopaque ice cloud if it passes the test and warm liquid water cloud if it fails the test (Pavolonis et al. 2005). There is one additional cloud type that has been included since Pavolonis et al. (2005). Overshooting cloud type is now determined if the emissivity of the cloud is close to 1 at the tropopause (personal correspondence, Andrew K. Heidinger 2010).

This study uses ascending and descending node data together. Low cloud fraction for this study is computed as the difference in total cloud fraction and mid-to-high level cloud fraction. Total cloud fraction in general is computed as the number of cloudy pixels (i.e. all cloud types) divided by the total number of pixels in the specified grid area. Mid-to-high level cloud fraction is defined as clouds that are opaque ice, cirrus, overlap, mixed-phase, or overshooting from 700 mb to the top of the atmosphere divided by the total number of pixels in the specified grid area. Low cloud fraction is then computed into monthly means for each month for each year.

b. GCM data

1. Models

The GCM datasets used in this study are from the GFDL/CM2.0 model (CM2) developed by the Geophysical Fluid Dynamics Laboratory of the National Oceanic and Atmospheric Administration and the NCAR/CCSM3.0 model (CCSM3) developed by the National Center for Atmospheric Research (Delworth et al. 2006, Collins et al. 2006a). These are both coupled climate models that were used in several simulations for the Intergovernmental Panel on Climate Change Fourth Assessment Report (IPCC AR4). These models in particular were selected because LTS was incorporated into the cloud parameterization scheme for CCSM3. CM2 does not use the LTS relationship. Having both allows for a more robust analysis of the LTS relationship in models. The data is freely available and was obtained from each models' data output website. Once downloaded, the

same 20°x20° grid box and time period as the PATMOS-x dataset were selected for comparisons.

2. Experiments

Two experiments were used with one realization for each: Climate of the 20th Century Experiment (20C3M) and 720 ppm Stabilization Experiment (SRESA1B). In the United States, the 20C3M experiment consisted of six simulations that were run from different initialization times (every 20 years) in the Pre-Industrial Control Run (PIcntrl). The data for this study comes from the first simulation of the 20C3M which started from the control run at year 360. Forcing variables included in this experiment are sulfate, solar, volcanoes, ozone, greenhouse gasses, halocarbons, black carbon, sea salt, and dust (CESM).

SRES stands for Special Report on Emissions Scenarios from the IPCC. There are four scenarios in the report that each incorporates different economic, demographic, and technological driving mechanisms. SRESA1B refers to a scenario (year 2000 – 2300) in which there is rapid economic growth, a mid-century population peak, and a balance across all fossil and non-fossil energy resources (IPCC-AR4). This particular scenario is selected because a recent report shows that observed carbon dioxide emissions from 1990-2008 are very close to the carbon dioxide emissions predicted by SRESA1B (Manning et al. 2010).

c. NCAR/CCSM3.0

1. Description

The components of the CCSM3 system include the Community Atmosphere Model version 3 (CAM3), the Community Land Surface Model version 3 (CLM3), the Community

Sea Ice Model version 5 (CSIM5), and an ocean component based upon the Parallel Ocean Program version 1.4.3 (POP) (Collins et al. 2006a). A flux coupler is used to bridge communication among the four component models and all five parts are run by five independent programs. The flux coupler provides flux boundary conditions and physical state information to each model as well as maintaining flux conservation among components. Boundary fluxes include momentum, water, heat, and salt and physical state information includes temperature, salinity, velocity, pressure, humidity, and air density (Collins et al. 2006a).

The standard configuration of CCSM3 used in the IPCC AR4, also known as the high resolution configuration, combines the T85 CAM3/CLM3 with the 1° POP/CSIM5. The T85 CAM3 refers to the Eulerian spectral dynamical core of CAM3 with triangular spectral truncation at 85 wavenumbers that corresponds with the 1.41° zonal resolution at the equator and 26 vertical levels. CLM is integrated on the same horizontal grid as CAM3. The 1° POP refers to the horizontal resolution of 1° in the ocean model. This also corresponds to a depth coordinate of 40 levels, 320 zonal points, 384 meridional points and CSIM5 is integrated on the same horizontal grid. In this high resolution configuration, fluxes and state information are exchanged every hour through the coupler from CAM3, CLM3, and CSIM5 and only once per day from POP. Each component has a separate internal time step of 20 minutes, 10 minutes, 1 hour, and 1 hour, respectively (Collins et al. 2006a).

2. Variables

Low cloud fraction was the variable used and was obtained from the Earth System Grid (http://www.earthsystemgrid.org/home.htm) which is the output data gateway for the

various CCSM3 experiments. CAM3 calculates three cloud fraction levels: low, middle, and high. The levels are defined by pressure levels: surface to 700 mb, 700 mb to 400 mb, and 400 mb to model top, respectively (Collins et al. 2004). A thorough comparison requires an understanding of how the model derives low cloud fraction.

CAM3 is the component model that generates cloud fraction from diagnostic relationships for amounts of three cloud types: low-level marine stratus, convective, and layered cloud (Collins et al. 2006b). Convective clouds are separated into shallow and deep schemes and are related to updraft mass flux. Layered clouds are defined when the relative humidity exceeds a specific value which varies according to pressure. Equations and more detail on these clouds types in CAM3 can be found in Collins et al. (2004). For the purposes of this study, we will only look at model parameterization of low-level marine stratus assuming it is the dominant cloud type in low cloud fraction though it is important to note that some of the other cloud types might also be classified as low cloud fraction. Klein and Hartmann's theory of LTS is the basis for low-level marine stratus cloud parameterization in CAM3 shown below (Collins et al. 2006b).

$$C_{st} = \min\{1., \max[0., (\theta_{700} - \theta_s) * .057 - .5573]\}$$

Bear in mind that the CAM3 uses the maximum-random (M/R) vertical cloud overlap scheme for radiation calculations and diagnostic purposes when determining low, medium, and high cloud fraction levels (Collins et al. 2004). The grid cell in GCMs is much larger than cloud elements, so capturing the vertical correlations between clouds requires an overlap assumption. Figure 7 provides a visual example of how the overlap assumption works.

In the version of M/R for radiation calculations, the number of random-overlap interfaces and a vector of pressures at each interface are input to the calculations. Maximally overlapped clouds are clouds in adjacent layers while randomly overlapped clouds are groups of clouds separated by one or more clear layers. In random overlap, the vector of pressures equals the pressure values at the bottom of each model level and the number of interfaces equals the number of model levels. In maximum overlap, the interface number equals one and the vector of pressures equals the pressure at that interface which is set to a value larger than the surface pressure. The version of M/R for diagnostic purposes uses maximum overlap by setting the number of interfaces equal to three and the vector of pressures equal to the pressures at the lower boundaries of each region. These parameters are determined for each grid cell at each time step (Collins et al. 2001).

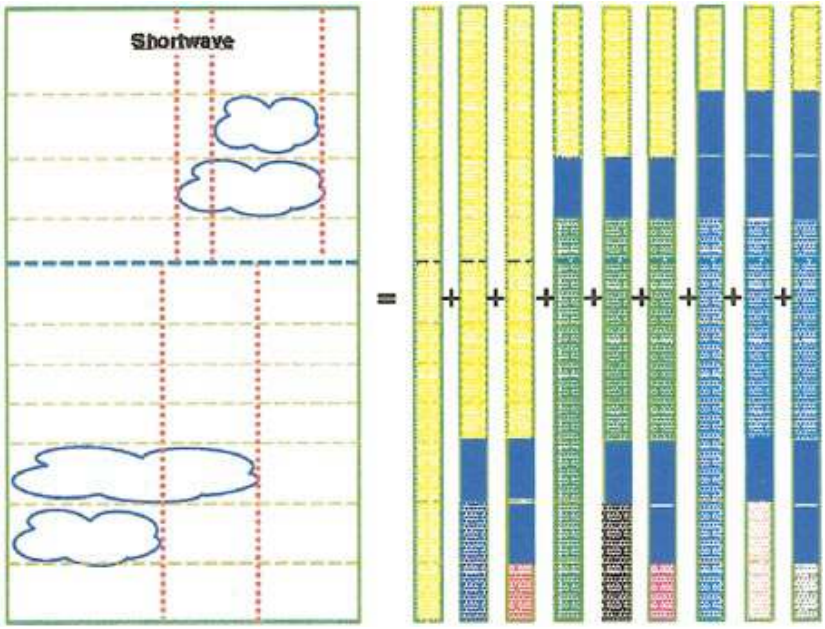

Figure 7. From Collins et al. (2001): "An example of the conversion of a vertical profile of partial cloud amounts to an equivalent set of binary cloud configurations. The overlap is assumed to be M/R with M overlap between clouds in adjacent layers and R overlap between groups of clouds separated by clear sky. The stippled color coding of layers in the binary cloud configurations indicates which configurations share identical radiative properties for downwelling direct and diffuse shortwave radiation at a given layer. The solid blue regions are clouds."

LTS for CCSM3 was calculated from air temperature and pressure variables obtained in the same manner as low cloud fraction. The temperature was recalculated from hybrid sigma pressure coordinates to sigma pressure coordinates (See Figure 8) (Collins et al. 2006a). Then the values for 700 mb and 1000 mb were used to calculate potential temperature at these levels by the following adiabatic equation: $\theta = T\left(\frac{P_o}{P}\right)^k$ where k is the dimensionless constant 0.286 (specific gas constant divided by the specific heat at constant

pressure) (Salby 1996). The potential temperature at 1000 mb was then subtracted from the potential temperature at 700 mb.

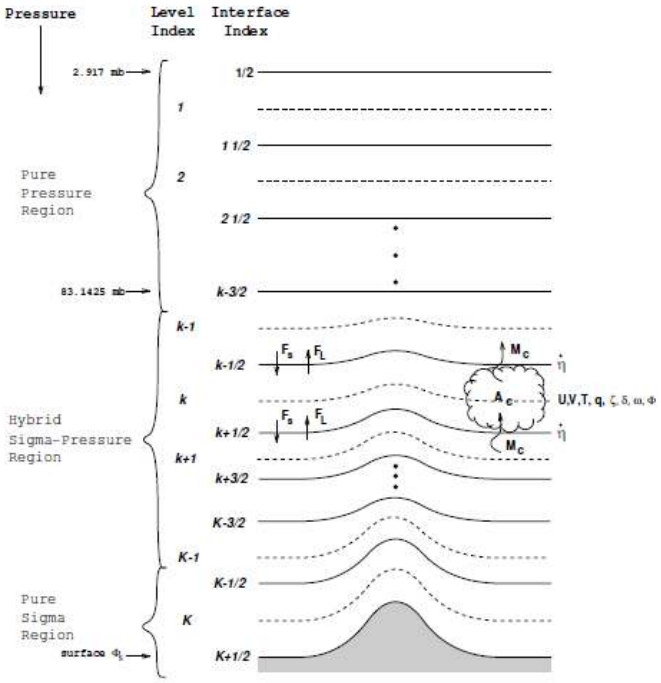

Figure 8. An illustration of CAM3 vertical structure from Collins et al. (2004).

d. GFDL/CM2.0

1. Description

The GFDL/CM2.0 model is composed of an atmospheric model (AM2.0), a land model (LM2.0), a sea ice model (SIS) and an ocean model (OM3.0) which communicate through a flux coupler every hour (Delworth et al. 2006). AM2.0 (herein referred to as AM2) uses a finite-difference dynamical core with a horizontal resolution of 2° latitude x 2.5° longitude and 24 vertical levels. The lowest 1.5 km has 9 vertical levels which makes the

resolution finer (Anderson et al. 2004). OM3.0 has 50 vertical levels and 1° horizontal grid spacing (Wittenberg et al. 2006).

2. Variables

Low cloud fraction was the variable obtained from the GFDL website, http://nomads.gfdl.noaa.gov/CM2.X/CM2.0/available_data.html. AM2 calculates three cloud fraction levels: low, mid, and high. The levels are defined by pressure levels: surface to 700 mb, 700 mb to 400 mb, and 400 mb to model top, respectively, and computed from cloud fraction predicted at each model level (personal correspondence, Chris Golaz of GFDL 2010).

AM2 predicts convective cumulus, boundary layer, and stratiform cloud types (Tiedtke 1993). Again, we will only look at model parameterization of low-level marine stratus assuming it is the dominant cloud type in the low cloud fraction variable, bearing in mind that some of the other cloud types might also be classified as low cloud fraction. The computation for cloud fraction is much more complicated than in CCSM3. Cloud fraction is "treated as a prognostic variable with sources and sinks based upon the equations in Tiedtke 1993" (personal correspondence, Stephen A. Klein of Program for Climate Model Diagnostics and Intercomparison 2010). AM2 assumes random overlap for clouds (Anderson 2004). This is defined by the equation $C_{\text{rand}} = c_{\text{a}} + c_{\text{b}} - c_{\text{a}}c_{\text{b}}$, where c_{a} is the cloud cover of the lower level and c_{b} is the cloud cover of the upper level (Hogan and Illingworth 2000).

LTS for CM2 was calculated from air temperature obtained from the Program for Climate Model Diagnosis and Intercomparison (PCMDI) multi-model database found online at https://esg.llnl.gov:8443/home/publicHomePage.do. The temperature was already

converted to sigma coordinates so the conversion to potential temperature was applied and the difference between 700 mb and 1000 mb was taken to calculate LTS.

e. NCEP/Reanalysis

The National Center for Environmental Prediction (NCEP) and NCAR reanalysis derived data for potential temperature is used in this paper to calculate observed LTS and is obtained from the website, http://www.esrl.noaa.gov/psd/. NCEP/Reanalysis was chosen because it has been used in other recent studies of low cloud fraction and LTS (Zhang et al. 2010, Ghate et al. 2009). This observed quantity is used for comparison to PATMOS-x and the GCM output. Monthly data is computed from data four times a day that has been averaged. The model uses a T62 core with horizontal resolution of 210 km (~2°) and 28 vertical levels. Potential temperature data for 700 mb and 1000 mb pressure levels were extracted and their difference taken in order to obtain LTS (Kalnay et al. 1996).

III. PATMOS-x/Model Comparisons

a. Low Cloud Fraction

The following boxplots (Figure 9) present low cloud fraction for PATMOS-x, CCSM3, and CM 2. There is a difference in time series for the GCM models for each experiment. For CCSM3, 20C3M spans years 1982 – 1999 and SRESA1B spans 2000 – 2009. CM2 spans 1982 – 2000 for 20C3M and 2001 – 2009 for SRESA1B. In order to compare all three datasets, year 2000 was eliminated. Thus, the plots are divided into pre- and post- 2000.

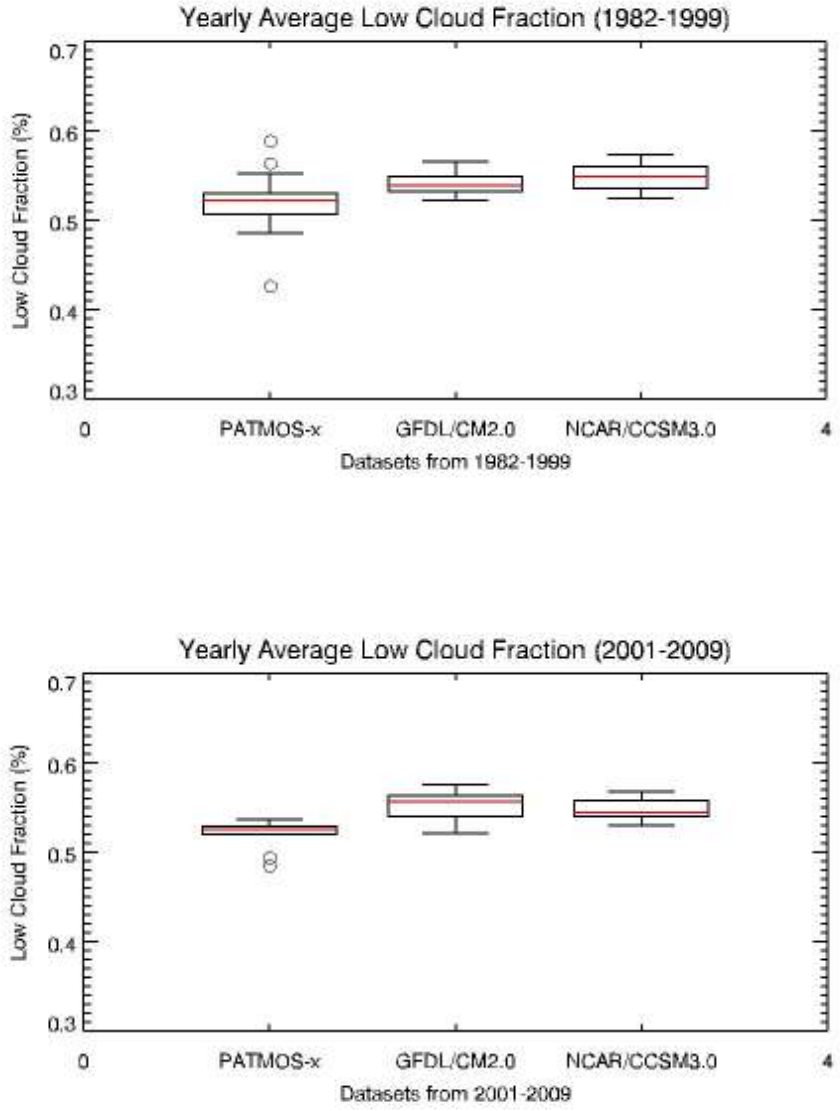

Figure 9. Boxplots showing yearly means of low cloud fraction for a) pre-200 and b) post-2000. The median (red line), interquartile range (box), minimum and maximum values, and outliers (circles) illustrate the differences among the three datasets, particularly CCSM3.

Figure 9 shows that overall both models simulate low cloud fraction reasonably well. CM2 is slightly closer to the observed low cloud fraction shown in the PATMOS-x dataset pre-2000 and CCSM3 is closer in post-2000. There is a minimal difference among the model/satellite biases for pre- and post- 2000. Total low cloud fraction ranges from approximately 48%-56% for PATMOS-x, 52%-57% for CM2, and 53%-57% for CCSM3 in years 1982-1999. For years 2001-2009 the total low cloud fraction is approximately 52%-54% for PATMOS-x, 52%-58% for CM2, and 53%-57% for CCSM3. Overall, the variability in both models is very similar and both are slightly higher than PATMOS-x.

It is also important to compare the data seasonally to determine if certain models simulate low cloud fraction seasonality similarly to the remotely-sensed observations. Figures 10 a, b, c, and d show seasonal means for 4 seasons (JFM, AMJ, JAS, OND) over the pre- and post- 2000 time spans. The models show different biases seasonally compared to interannually and each model simulates two seasons fairly well. CM2 JFM and JAS correlate better with PATMOS-x than CCSM3 for both pre and post-2000 (Figure 10a and 10c, Table 2). Likewise, CCSM3 AMJ and OND correlate better with PATMOS-x than CM2 pre and post-2000 with the exception of post-2000 OND (Fig 10b and 10d, Table 2). The JAS and OND seasons have been shown to contain the highest amount of low cloud in this particular region (KH93, Jensen et al. 2008), thus it is encouraging to see the pre and post-2000 simulations capture low cloud fraction well. The strongest seasonal biases exist in CCSM3 JFM and CM2 AMJ.

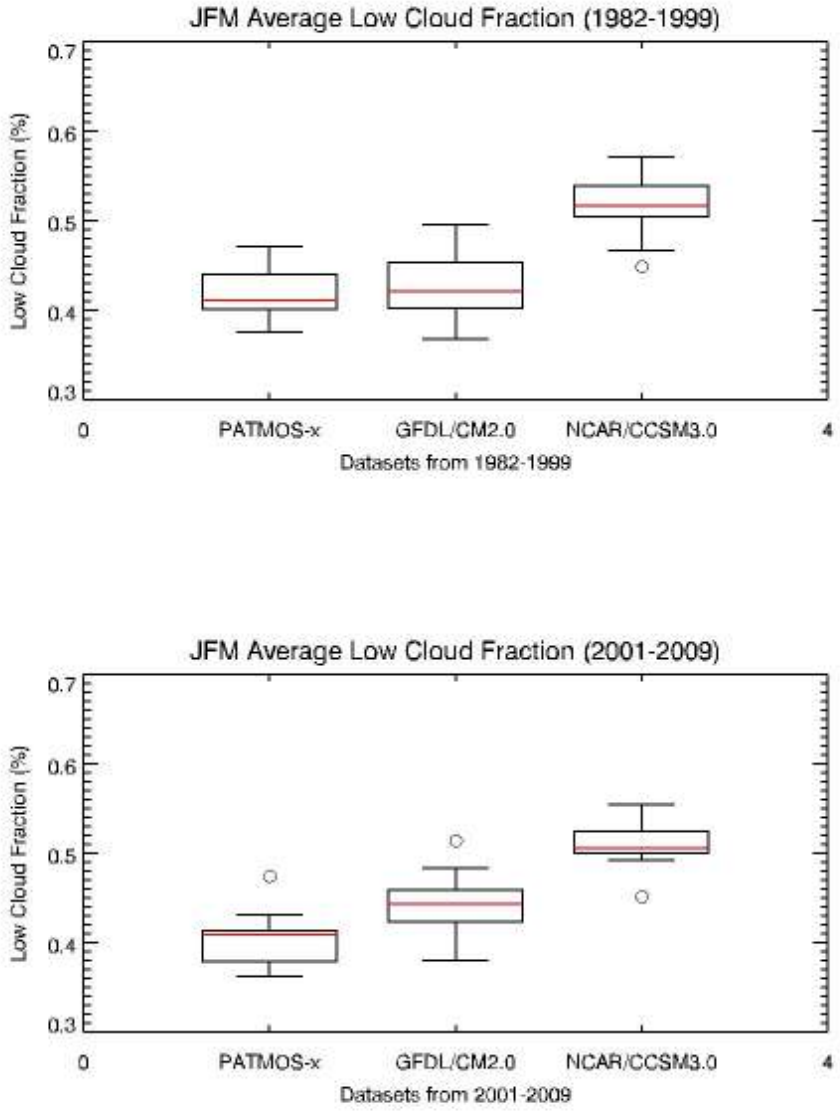

Figure 10a. January, February, and March (JFM) seasonal means for each dataset. This shows a close relationship between PATMOS-x and CCSM3 while CM2 is very far off in both time series.

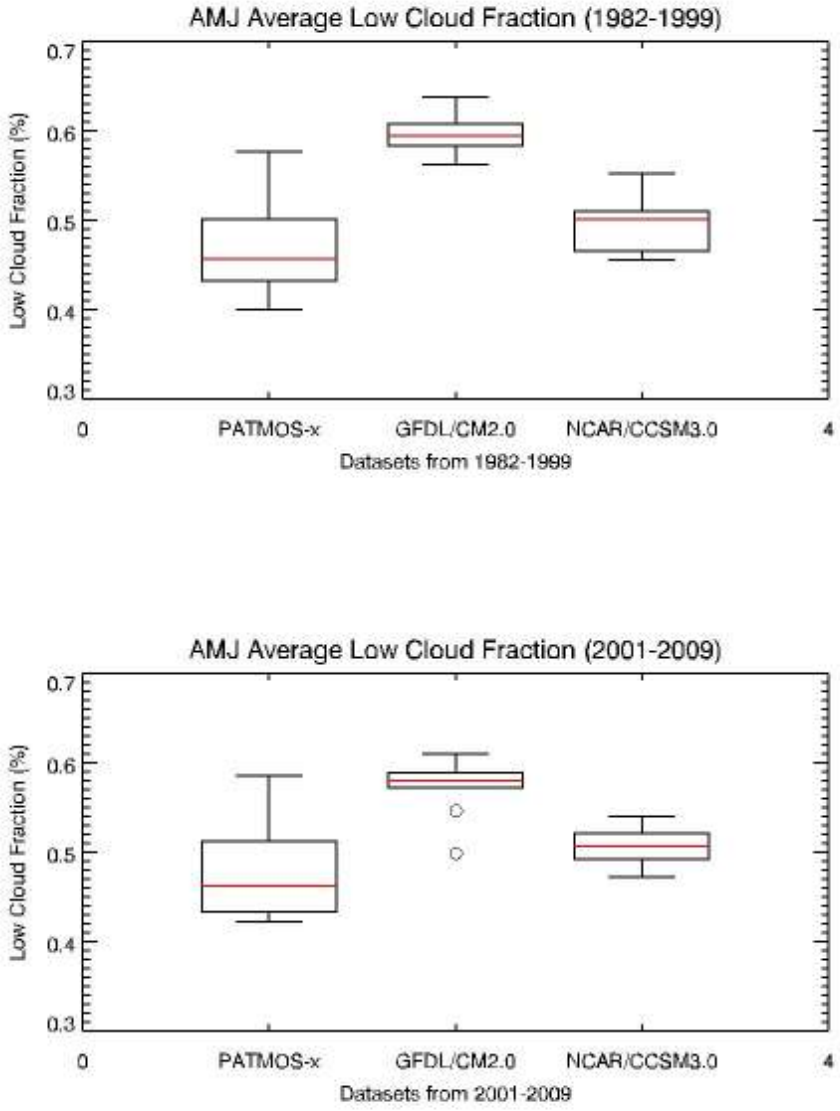

Figure 10b. April, May, and June (AMJ) seasonal means for each dataset. PATMOS-x and CM2 are closer in both time series.

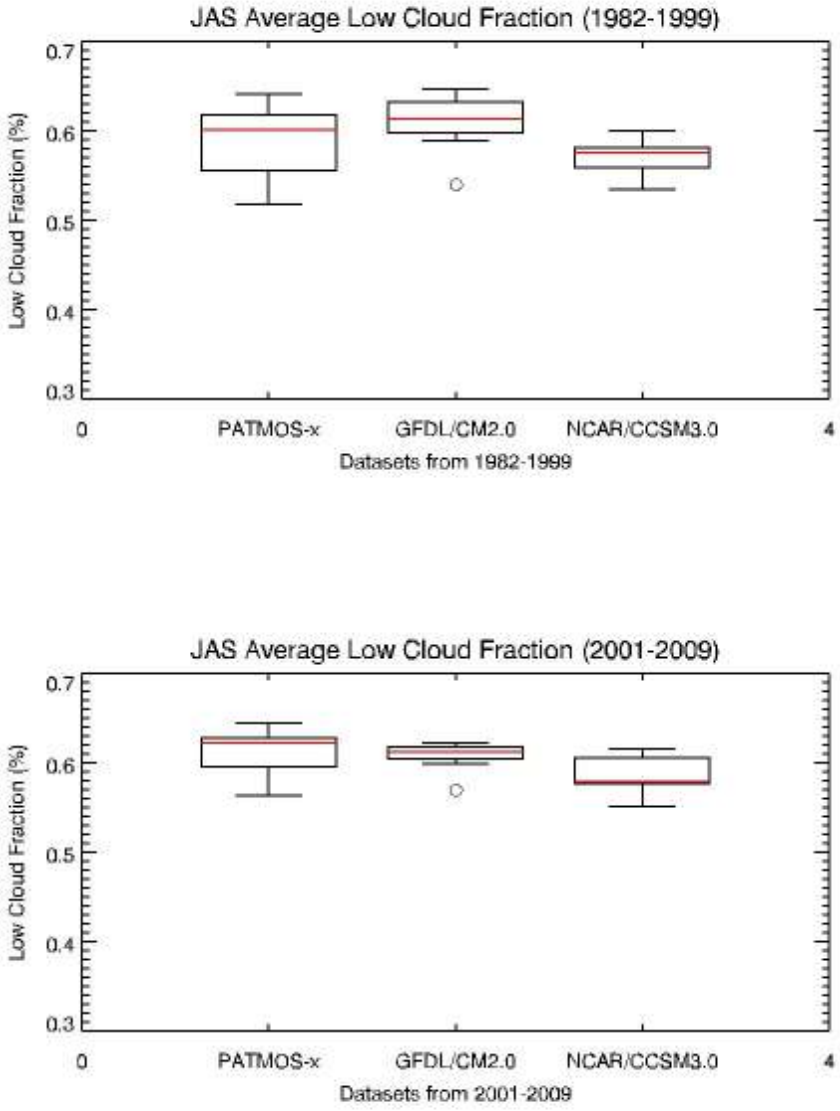

Figure 10c. July, August, and September (JAS) seasonal means for each dataset. CM2 has a closer relation to PATMOS-x pre-2000, but neither model represents low cloud fraction well post-2000.

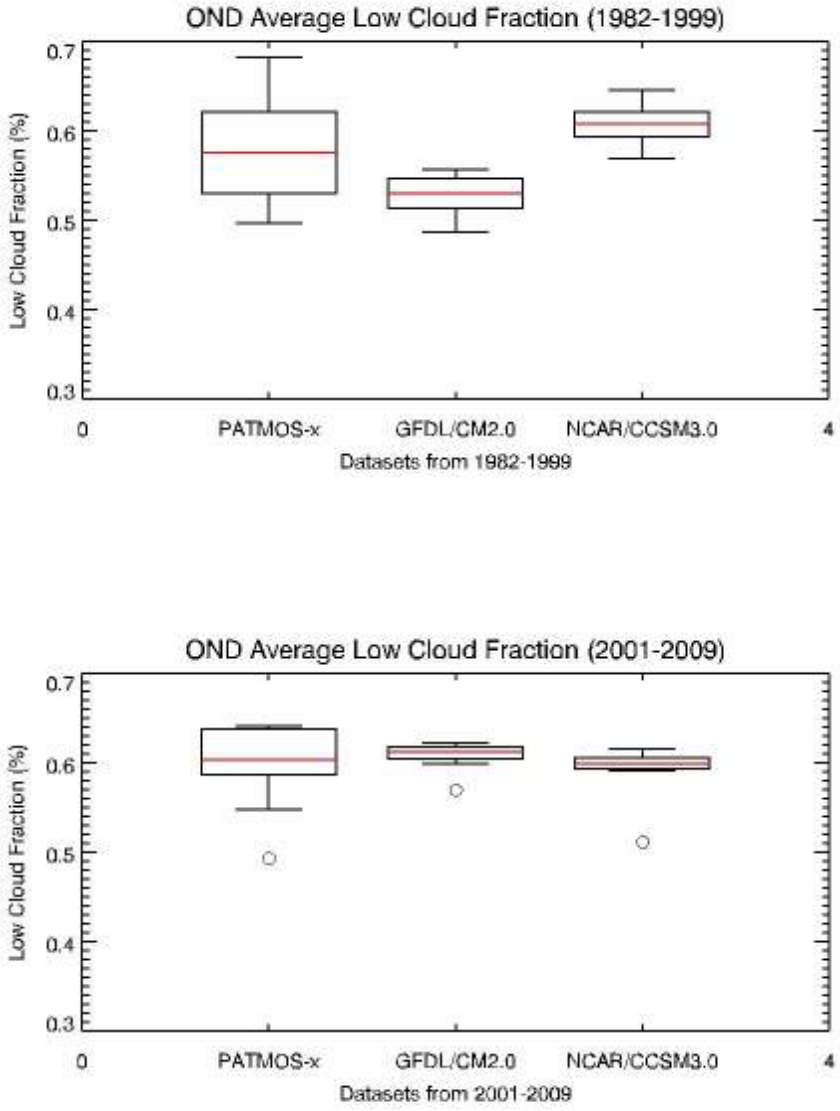

Figure 10d. October, November, and December (OND) seasonal means for each dataset. CM2 and PATMOS-x have a very close relationship for this season while CCSM3 is very different.

Table 2. Pearson correlation coefficients (r) of seasonally averaged PATMOS-x and model data for low cloud fraction (Figures 9 and 10a-d). Boxes highlighted in yellow indicate high significance ($p<0.01$) and boxes highlighted in blue indicate significance ($p<0.05$).

	PATMOS-x vs. CCSM3		**PATMOS-x vs. CM2**
Pre-2000 Annual	r = -0.281	**Pre-2000 Annual**	r = -0.424
Post-2000 Annual	r = -0.268	**Post-2000 Annual**	r = -0.120
Pre-2000 JFM	r = -0.013	**Post-2000 JFM**	r = -0.185
Post-2000 JFM	r = 0.074	**Post-2000 JFM**	r = 0.235
Pre-2000 AMJ	r = 0.061	**Pre-2000 AMJ**	r = -0.021
Post-2000 AMJ	r = 0.466	**Post-2000 AMJ**	r = 0.006
Pre-2000 JAS	r = 0.218	**Pre-2000 JAS**	r = -0.244
Post-2000 JAS	r = -0.007	**Post-2000 JAS**	r = -0.395
Pre-2000 OND	r = -0.357	**Pre-2000 OND**	r = -0.231
Post-2000 OND	r = -0.084	**Post-2000 OND**	r = 0.375

This table shows correlations for low cloud fraction to better understand the relationships represented in the previous boxplot figures. Pre-2000, CM2 is a highly significant ($p<0.01$) predictor of low cloud cover annually which is suggested in Figure 9. This is an interesting result considering the lack of LTS in the cloud parameterization scheme for CM2. Pre-2000 OND for CCSM3 is the only season with a significant correlation, surprisingly (Figure 10d). Overall, there is only one significantly correlated season which does not help explain the interannual variability in low cloud fraction between observations

and models or why CM2 is highly correlated pre-2000. There do seem to be seasons where different models simulate low cloud fraction more accurately. This emphasizes the fact that seasonality can be a large factor in model simulations and that other large scale phenomena could be influencing the seasonal pattern such as the El Nino Southern Oscillation (ENSO), changes in aerosol loading in the region, or changes in LTS which is the focus of this study (Ghate et al. 2009).

b. Low Cloud Fraction and LTS Comparisons

1. PATMOS-x and NCEP-LTS

Given the known relationship between LTS and low cloud fraction, linear regression can reveal how this relationship varies among the observations and models and whether these differences reveal the cause of observation-model biases. The regressions here are done by season due to the large seasonal variability in LTS and low cloud fraction. Figures 11 a, b, c, and d show PATMOS-x and LTS as calculated from NCEP/Reanalysis potential temperature data. The plotted points are seasonal mean values for each year (1 value per year). The time spans are 1982-1999 (pre-2000) and 2000-2009 (post-2000).

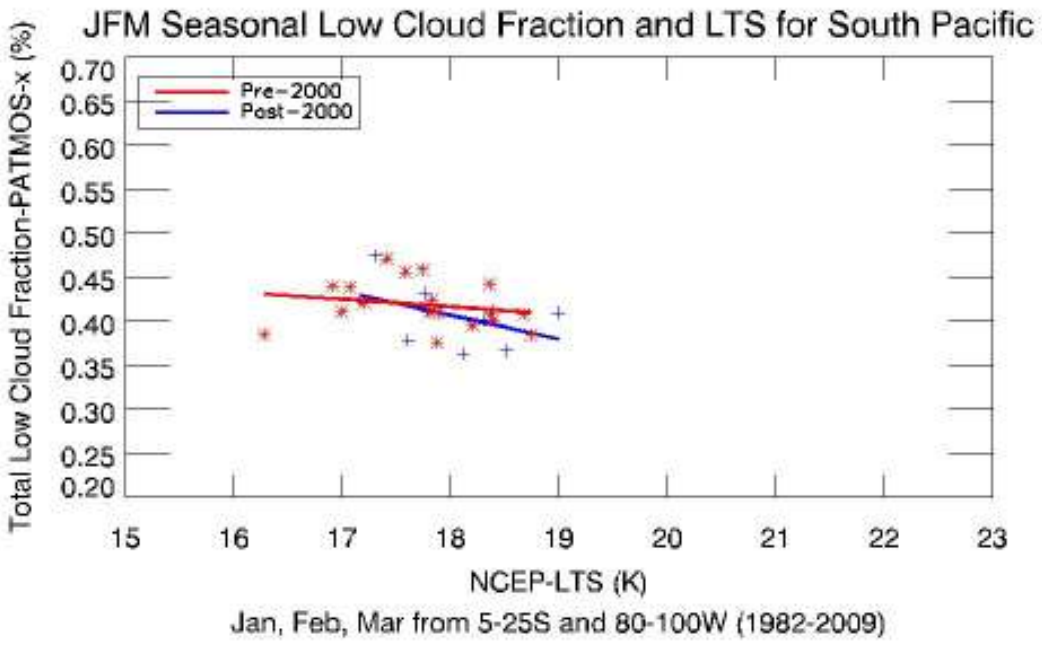

Figure 11a. JFM seasonal mean values of low cloud fraction and LTS. Cloud fraction is between ~35% and ~48% with LTS primarily ranging from ~16 K to ~19 K.

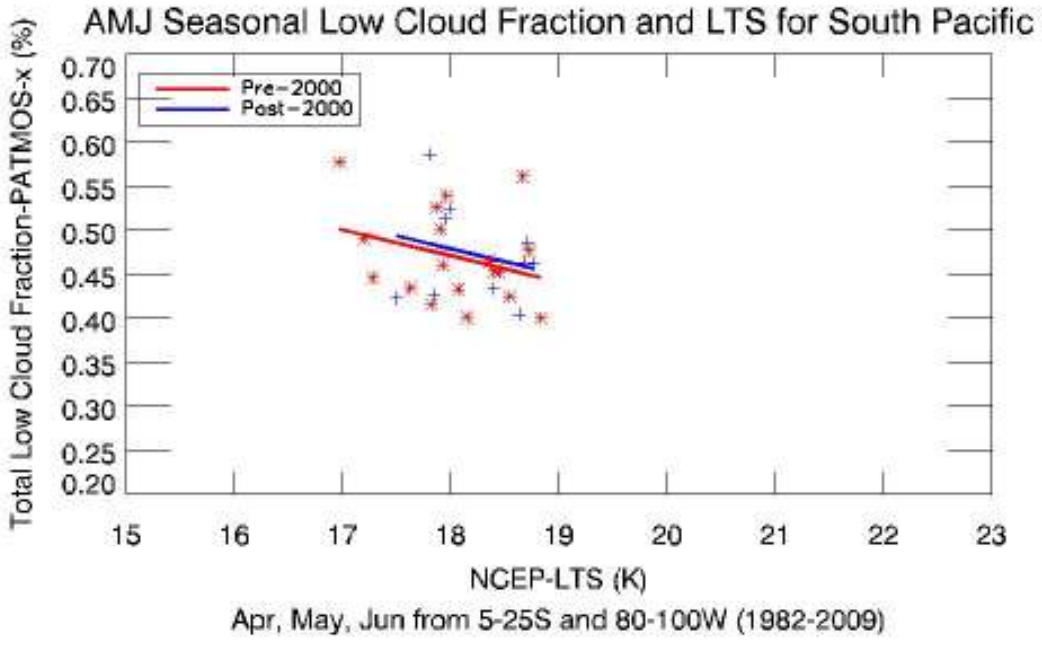

Figure 11b. AMJ seasonal mean values of cloud fraction and LTS. Cloud fraction is between ~38% and ~60% with LTS values of ~17 K to ~19 K.

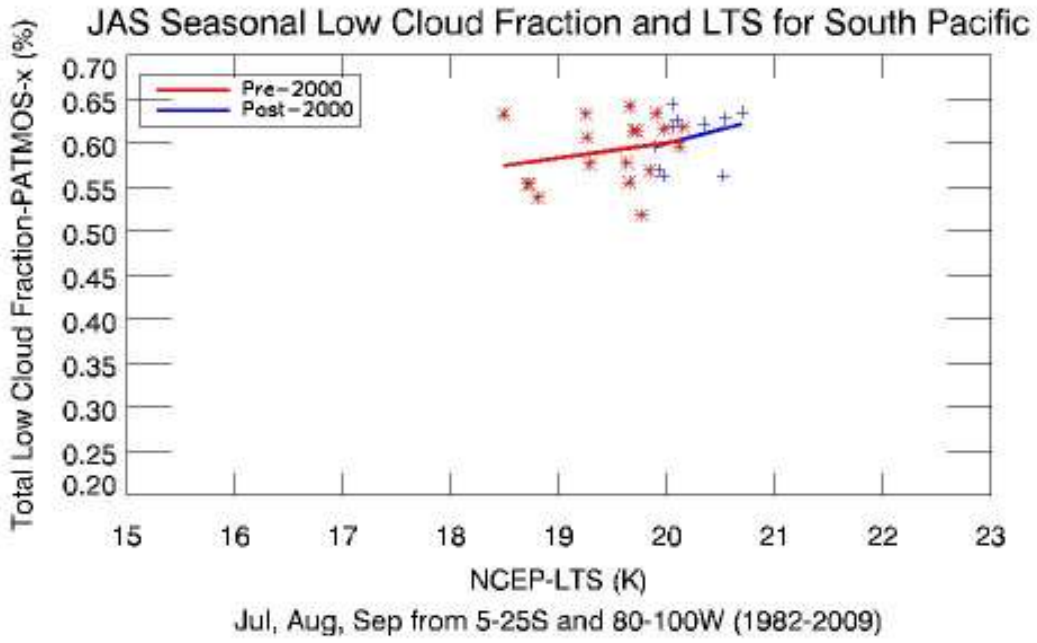

Figure 11c. JAS seasonal mean values of cloud fraction and LTS. Cloud fraction is higher overall than in previous seasons from ~50% to ~65% with higher LTS values from ~18.5 K to ~21 K.

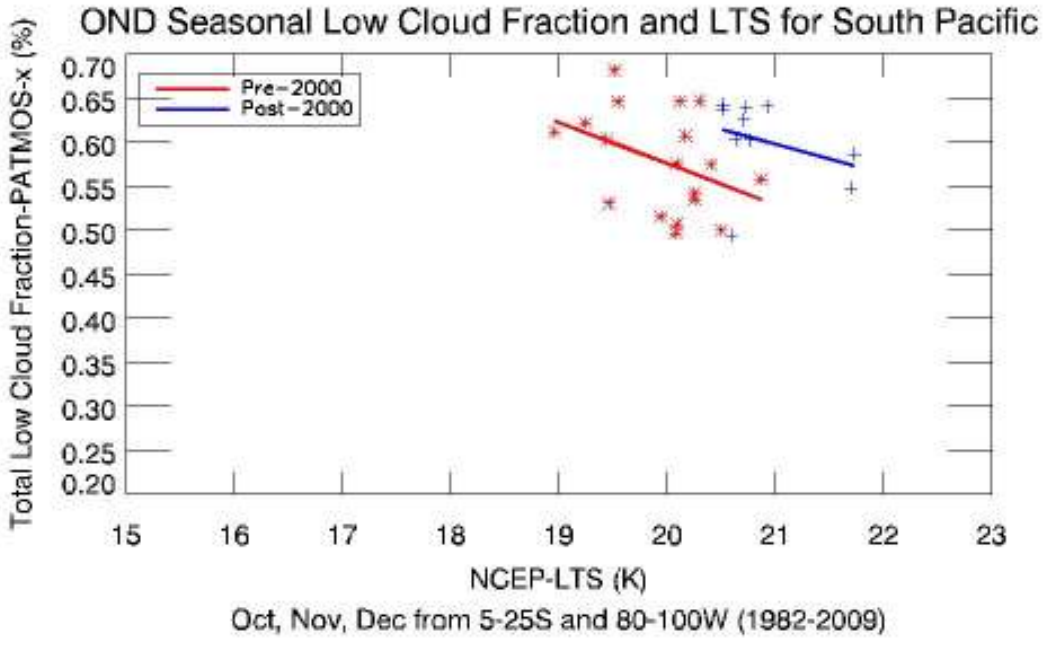

Figure 11d. OND seasonal mean values of cloud fraction and LTS. Cloud fraction ranges from ~48% to ~70% while LTS values are ~19 K to ~22 K.

The following table contains calculated values for the slope (a) of the regression line and values for the Pearson correlation coefficient (r) for each of the 4 figures.

Table 3. Regression values for Figures 11 a, b, c, and d for PATMOS-x and NCEP-LTS. Boxes highlighted in blue indicate significance ($p<0.05$).

	Figure 11a	**Figure 11b**	**Figure 11c**	**Figure 11d**
Pre-2000	a = -0.009	a = -0.030	a = 0.017	a = -0.047
	r = -0.210	r = -0.301	r = 0.233	r = -0.397
Post-2000	a = -0.027	a = -0.029	a = 0.031	a = -0.033
	r = -0.465	r = -0.249	r = 0.294	r = -0.311

These figures indicate interesting seasonal trends that change pre and post-2000 particularly for JFM, and OND. From the data in Table 3, the correlation between PATMOS-x and LTS post-2000 is significant ($p<0.05$) for JFM and pre-2000 OND is also significant. This indicates that there is a trend in LTS vs. PATMOS-x for these seasons. Even more interesting is the negative correlation for JFM, AMJ, and OND. This means that as LTS increases, low cloud fraction decreases which is the opposite of the relationship in KH93. Possible reasons for this discrepancy could be averaging over the study domain or not accounting for strong ENSO events. Further research should be conducted to better understand this seemingly opposite relationship.

JAS and OND show changing relationships in low cloud fraction and LTS. Though only pre-2000 OND is significant, there is a lot of variability within the season. Figure 11c illustrates the expected positive correlation between low cloud fraction and LTS. It also shows that LTS values pre-2000 range from about 18.5 K to 20 K while LTS values

post-2000 only range from 20K to 21K with overall higher low cloud fraction values from 55% to 65%. This suggests increased low cloud and LTS within the past 10 years to values that were never reached prior to 2000. Pre-2000 OND has a significant negative correlation with a fair amount of variability in low cloud fraction. Figure 11d shows LTS values pre-2000 between 19 K and 21 K and post-2000 LTS values between 20.5 K and 22 K. Additionally, low cloud fraction is higher overall post-2000 between 54% and 64% compares to pre-2000 at 48% to 68%. As in JAS, this suggests that low cloud and LTS have increased within the past 10 years, even if their correlation is negative.

2. CCSM3/CCSM3-LTS

Low cloud fraction from CCSM3 is plotted with the calculated LTS values from CCSM3. Since this cloud parameterization scheme directly incorporates LTS, it is expected that the two will be strongly correlated. Figures 12 a, b, c, and d are the same seasonal plots as in the previous 4 figures but for CCSM3. Table 4 contains the same information as Table 3 but for the following figures.

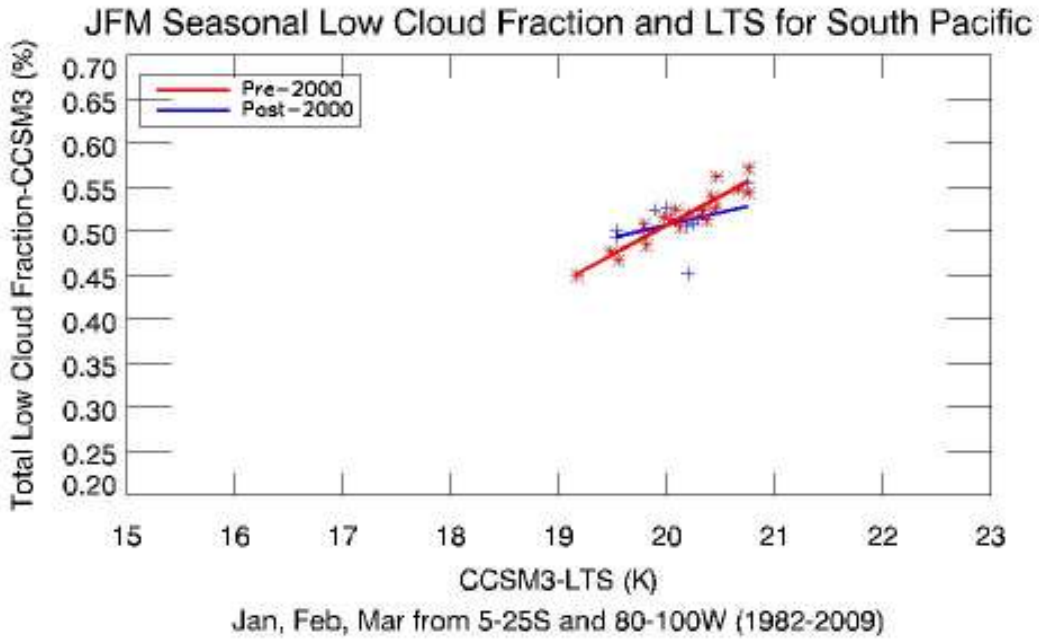

Figure 12a. JFM seasonal mean values of cloud fraction and LTS. Cloud fraction ranges from ~45% to ~58% and LTS values are ~19 K-21 K.

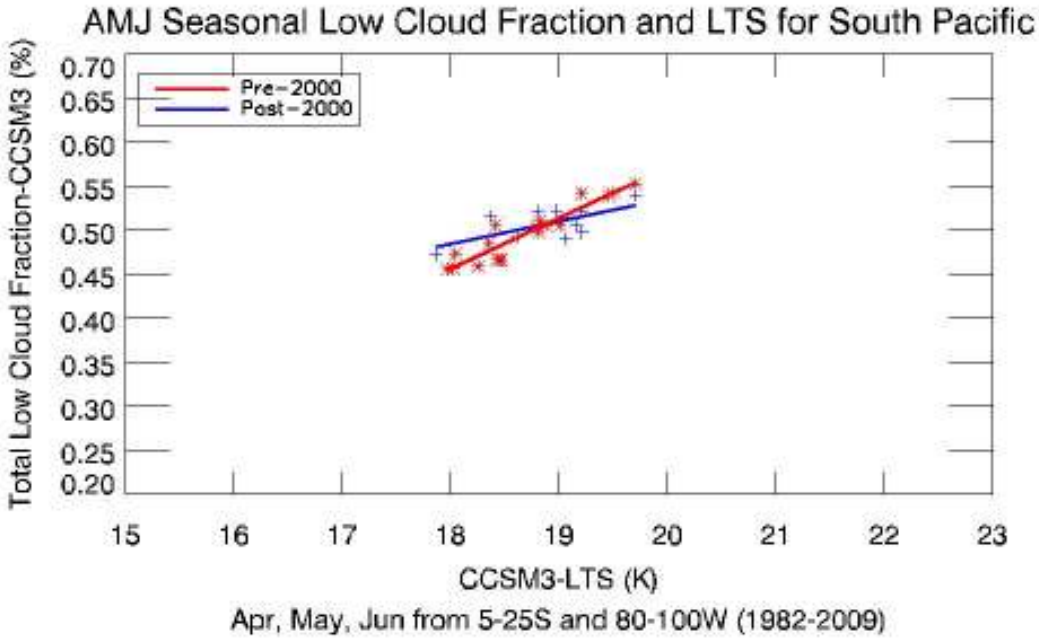

Figure 12b. AMJ seasonal mean values of cloud fraction and LTS. Values for cloud fraction are ~43% to ~55% while LTS values are ~17.8 K-19.8 K.

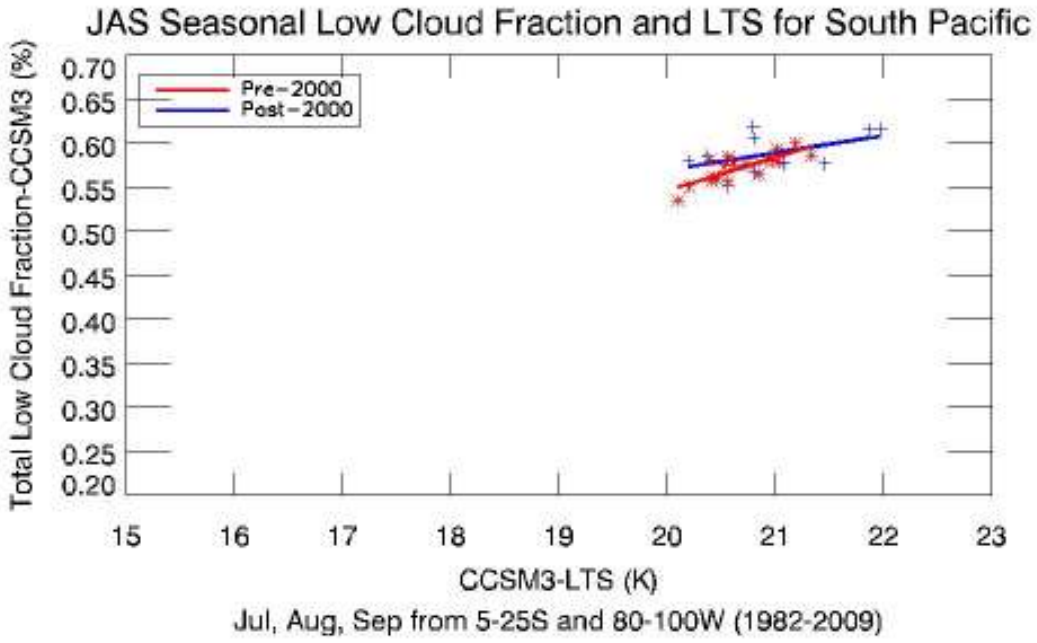

Figure 12c. JAS seasonal mean values of cloud fraction and LTS. Cloud fraction ranges from ~53% to ~64% range as the previous figures and LTS ranges from ~20 K-22 K.

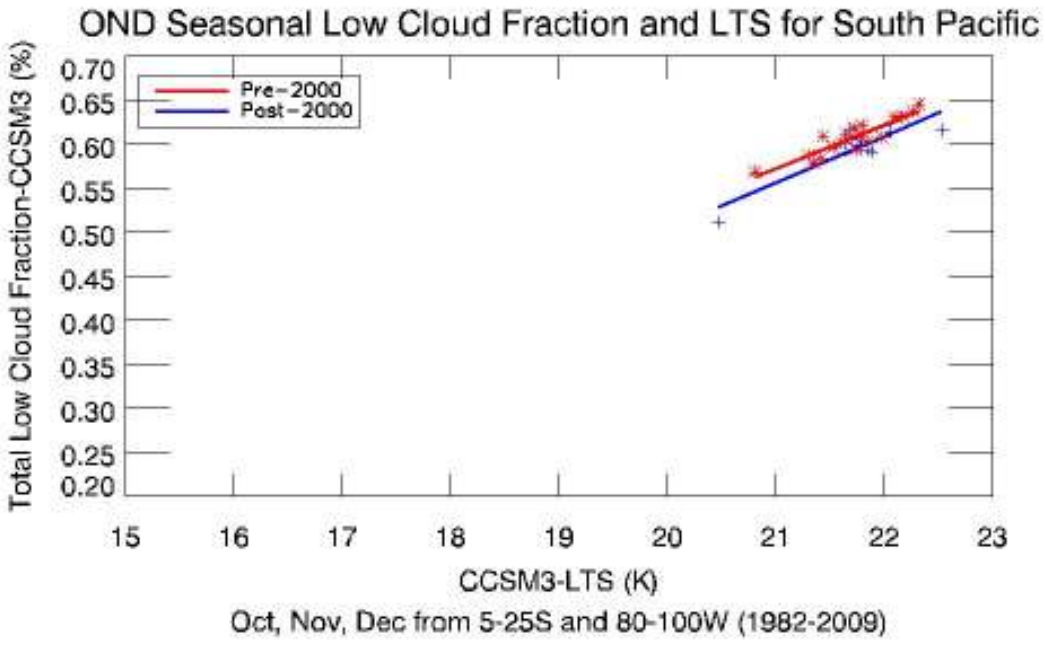

Figure 12d. OND seasonal mean values of cloud fraction and LTS. Cloud fraction values are ~45% to ~56% and LTS values are in a narrow cluster from ~20.5K-22.5K.

Table 4. Regression values for Figures 12 a, b, c, and d for CCSM3 and CCSM3-LTS. Boxes highlighted in yellow indicate high significance ($p<0.01$) and boxes highlighted in blue indicate significance ($p<0.05$).

	Figure 12a	**Figure 12b**	**Figure 12c**	**Figure 12d**
Pre-2000	a = 0.066	a = 0.058	a = 0.038	a = 0.036
	r = 0.931	r = 0.934	r = 0.795	r = 0.429
Post-2000	a = 0.029	a = 0.026	a = 0.020	a = 0.008
	r = 0.399	r = 0.654	r = 0.510	r = 0.199

There is strong correlation among all seasons pre-2000 and AMJ post-2000 ($p<0.01$). The correlation for all seasons is positive meaning as LTS increases, cloud fraction also increases. This is expected since the LTS relationship is incorporated into the cloud parameterization scheme. LTS values are slightly higher than observation ranging from 17.8 K to 22.5 K compared to 16 K to 22 K. It is also exactly opposite of the relationship observed in JFM, AMJ, and OND for PATMOS-x. JAS in Figure 12c is fairly similar to observation in Figure 11c in that post-2000 LTS (20 K-22 K) is greater than pre-2000 LTS (20 K-21 K) and low cloud fraction is higher overall post-2000 (55%-63%) compared to pre-2000 (53%-60%). This supports the idea shown in observation that there has been an increase in LTS and low cloud fraction within the past 10 years.

3. CM2/CM2-LTS

Low cloud fraction from CM2 is plotted with the calculated LTS values from CM2. Since CM2 runs 20C3M through 2000 and starts SRESA1B from 2001, the data is separated into pre- and post-2001. This cloud parameterization scheme does not directly incorporate LTS so it is expected that the two will not be strongly correlated. Figures 13 a, b, c, and d are the same seasonal plots as in the previous 4 figures. Table 5 contains the same information as Tables 3 and 4 but for the following figures.

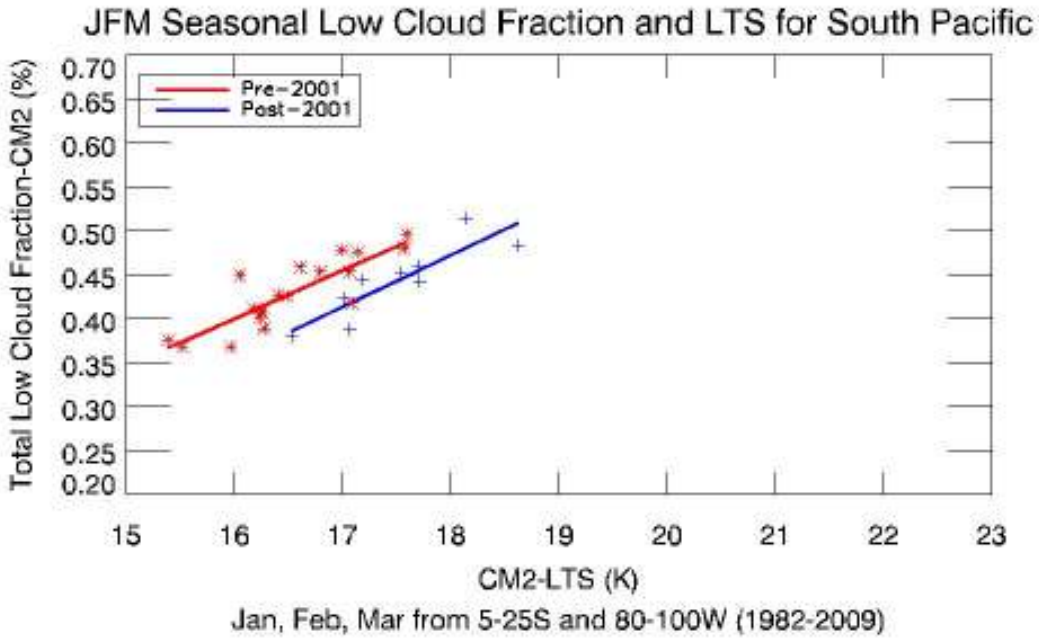

Figure 13a. JFM seasonal mean values of cloud fraction and LTS. Cloud fraction ranges from ~36% to ~53% and LTS values are ~15.5 K-19.8 K.

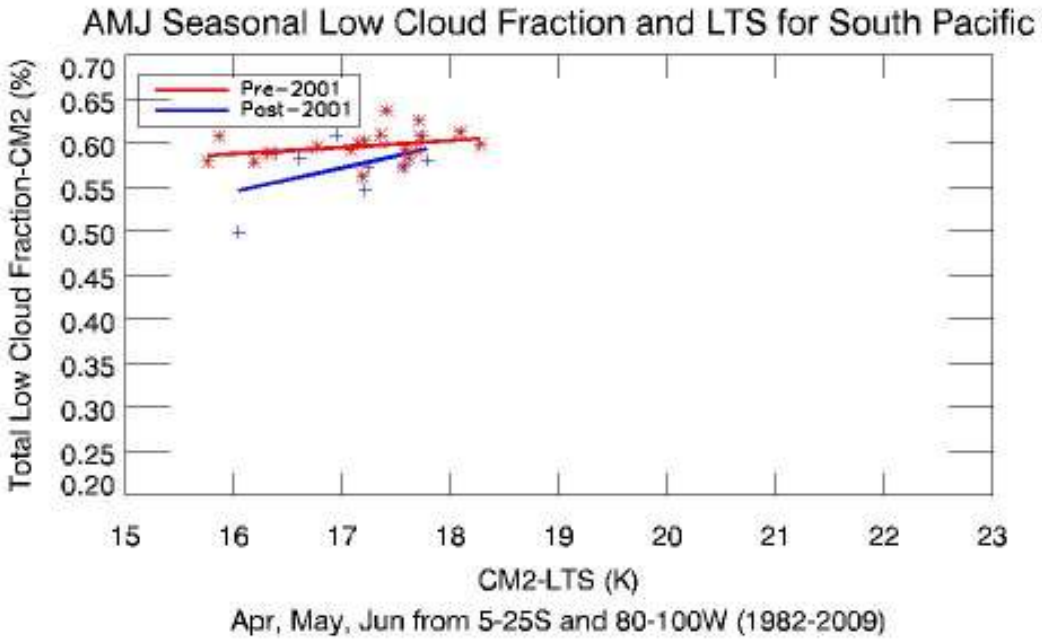

Figure 13b. AMJ seasonal mean values of cloud fraction and LTS. Cloud fraction values are ~50% to ~64% while LTS values are heavily concentrated from ~15.8 K-18.2 K.

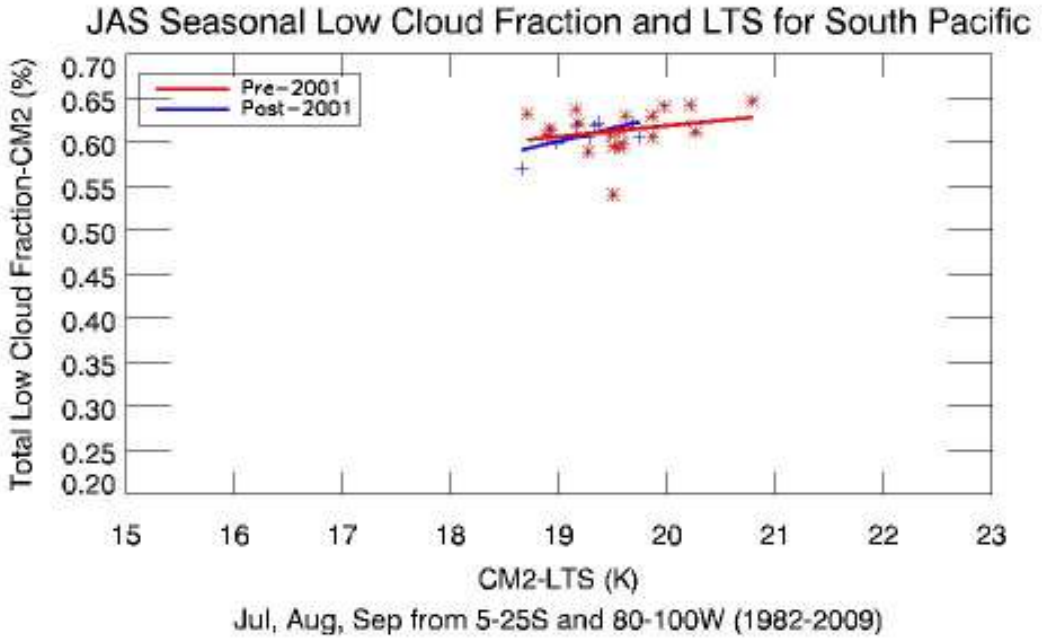

Figure 13c. JAS seasonal mean values of cloud fraction and LTS. Values of cloud fraction range from ~54% to ~65% and LTS ranges from ~18.5 K-20.8 K.

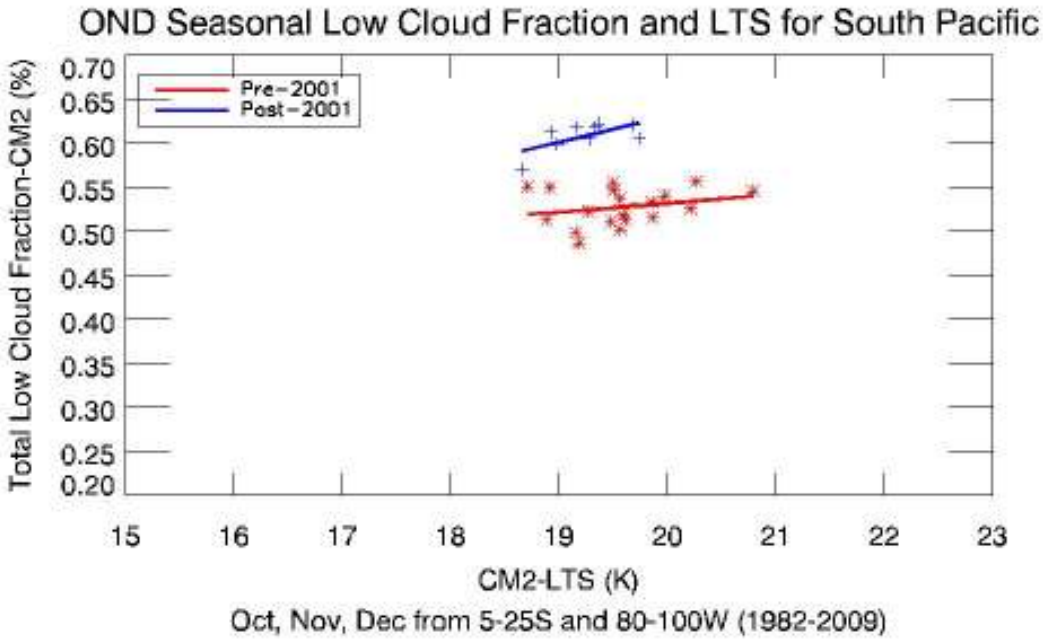

Figure 13d. OND seaonal mean values of cloud fraction and LTS. Cloud fraction ranges from ~48% to ~64% and LTS ranges from ~18.5 K-21 K.

Table 5. Regression values for Figures 13 a, b, c, and d for CM2 and CM2-LTS. Boxes highlighted in blue indicate significance ($p<0.05$) and boxes highlighted in yellow indicate high significance ($p<0.01$).

	Figure 13a	**Figure 13b**	**Figure 13c**	**Figure 13d**
Pre-2001	a = 0.055	a = 0.007	a = 0.012	a = 0.010
	r = 0.856	r = 0.290	r = 0.258	r = 0.244
Post-2001	a = 0.059	a = 0.027	a = 0.030	a = 0.030
	r = 0.876	r = 0.492	r = 0.643	r = 0.643

CM2 has one more year of values than pre-2000 PATMOS-x and one less year of values than post-2000 PATMOS-x. In that sense the two datasets cannot be compared exactly

one-to-one, however, the shift in date ranges is not believed to have a significant effect on the results. Surprisingly, all post-2001 seasons have a significant correlation between low cloud fraction and LTS even though LTS is not directly incorporated into the cloud parameterization scheme. Both pre and post-2001 JFM are highly correlated. This could suggest that excluding the LTS relationship from the cloud parameterization in the SRESA1B experiment run, simulates the LTS relationship well. However, low cloud fraction alone is not significant on a seasonal scale from Table 2 and Figures 10a-d. Low cloud fraction is significant pre-2000 for CM2. Thus, it is puzzling that the strong correlation in low cloud fraction and LTS post-2001 does not yield more significant results in low cloud fraction at a seasonal or interannual scale. Perhaps the high significance in the LTS relationship for pre-2001 JFM is driving the pre-2000 low cloud fraction significance. LTS values for CM2 are slightly lower than LTS values for PATMOS-x (15 K-21 K compared to 16 K-22 K). This could indicate that some other component of the model is keeping air temperature (from 700 mb to 1000 mb) cooler than observed.

All seasons have a positive correlation between low cloud fraction and LTS meaning as LTS increases, low cloud fraction also increases. This is the opposite of the observation data for JFM, AMJ, and OND but is the same as CCSM3. This suggests that LTS is not the only parameter driving seasonality in observations. JAS in Figure 13c does not show the same pattern as that in Figure 11c and Figure 12c. In CM2, LTS ranges between 18.5 K and 21 K for pre-2001 and 18.5 K and 20 K for post-2001. In observation and CCSM3 JAS seasons, LTS has increased post-2000 along with low cloud fraction. The fact that CCSM3 is also significant in this season gives more validity to the trend, especially since CM2 does not

incorporate the LTS relationship. However, the pattern in observation is more consistent with the pattern in CCSM3.

IV. Discussion/Conclusions

a. Re-evaluating the Low Cloud Fraction-LTS Relationships

-Is there a relationship between PATMOS-x low cloud fraction and NCEP-LTS that supports the initial empirical relationship first presented by Klein and Hartmann (1993)?

Given the seminal relationship first presented by KH93, it is surprising that this relationship does not appear to be consistent to what is observed in PATMOS-x low cloud fraction and NCEP-LTS. After all, from the plots of seasonal low cloud fraction and LTS (Figures 11a-d), there is definitely a visual correlation between the two, but the actual 1:1 correlation is poor and this further breaks down at the interannual and interseasonal scale. For two seasons, post-2000 JFM and pre-2000 OND, there is a significant correlation between PATMOS-x low cloud fraction and LTS. JAS for both time periods maintains the LTS relationship but the other three seasons show a different relationship than the one described in KH93 which says that increased LTS corresponds to increased low cloud fraction.

This lack of strong relationship could be attributed to several things. First, the data used in KH93was from a 30 year time period right before the time period used in this study. The relationship between low cloud fraction and LTS could have changed over past 28 years given ongoing anthropogenic climate change, though a clear mechanism to drive this is not clear. Additionally, their paper used surface observations from ships to calculate low cloud fraction whereas the data in this study is from polar orbiting satellites, and consequently, it may be the case that while KH93 observations preferentially sampled areas where low cloud fraction-LTS relationships are strong, and domain average observations by satellite fail to support this relationship over the entire study domain. Due to the larger size of the study

domain, ENSO could have a greater effect on the results of this study than KH93. Finally, both datasets could incorporate more than just low cloud due to the way in which they were calculated. PATMOS-x low cloud fraction was computed through various algorithms from a top-down perspective while KH93 used observers on ships from a bottom-up perspective to compute low cloud fraction. Additionally, the cloud amounts in KH93 were averaged seasonally to a resolution of 5°x5° which is much coarser than PATMOS-x (KH93).

An issue also arises with the calculation method for LTS. KH93 used data from the European Centre for Medium-Range Weather Forecasting (ECMWF) for years 1980-1987 to compute 700mb monthly temperatures. This study used NCEP/Reanalysis data for all years studied (1982-2009). It could be suggested that the LTS calculations in this study are more accurate simply because the temperatures were actually observed in the same time period as low cloud fraction. It is also important to remember that this region is larger than the region in KH93 which could account for this difference.

b. Model Assessment

-Do models accurately represent low cloud fraction at interannual and seasonal scales?

From Figure 9 and Table 2 it is apparent that both models are very similar in representing low cloud fraction on the long-term average. Pre-2000 interannual variation in CM2 low cloud fraction is significantly related to PATMOS-x. This suggests that the model is capturing interannual variability well, but some other process or factor in the calculation of cloud fraction keeps the values biased slightly high.

Seasonally, two out of the four seasons for each model simulate well the interannual variability observed by PATMOS-x. JFM and JAS for CM2 capture low cloud fraction variability better than CCSM3, however, AMJ and OND for CCSM3 capture low cloud

fraction variability better than CM2. However, post-2000 JFM (Figure 10c) shows a different pattern with both models overestimating low cloud fraction. The reason for this is unclear but could be due to the cloud parameterization schemes in the models not only in the sense of LTS relationship but in the use of different overlap assumptions.

-Do models show the same relationship between low cloud fraction and LTS as observations do?

Both models indicate some relationship between low cloud fraction and LTS on a seasonal scale, but the relationship is far different from observations in this study. CCSM3-LTS values are slightly higher than observations (~17.8-22.5 K compared to 16K-22 K) while CM2-LTS values are slightly lower than observations (~15-21 K) for both time periods. One conclusion may be that even though CCSM3-LTS is closer to observations which would be expected given the use of LTS in the cloud parameterization scheme, the values are still higher than observed suggesting that the cloud scheme is still missing something especially since there is almost a two degree difference in minimum LTS values. CM2-LTS did not use LTS in the cloud parameterization scheme and still resolved very close to the observed values for this quantity which is surprising. Also surprising is the significance of the trends in low cloud fraction and LTS per season found in CM2, despite the lack of LTS explicitly being used in the parameterization. A possible explanation is that LTS could be an emergent relationship arising from interactions of the cloud parameterization scheme with the boundary layer parameterization, but this warrants further scrutiny.

Both models do not simulate the same relationship shown in observations for low cloud fraction and LTS in JFM, AMJ, and OND. The slope of the relationship is exactly opposite of the trend found in observations from this study but it is the relationship expected from KH93 and others which generally shows an increase in LTS leading to an increase in low cloud fraction. Since the models simulate the relationship shown in other studies, the differences between them and observations in this study is more likely a result of the differences noted in part ***a*** of this section. JAS does exhibit the same relationship as observations though the relationship is only significant in the models.

-Does the NCAR/CCSM3 model simulate low cloud fraction more accurately than the GFDL/CM2 model since it incorporates LTS into its cloud parameterization scheme for low clouds?

This hypothesis cannot be supported by this study. While LTS has been shown to be a good predictor of low cloud fraction in other studies, CM2 was the model with a significant relationship pre-2000 with observation low cloud fraction interannually (Figure 9 and Table 2). One season, pre-2000 OND shows a significant relationship between CCSM3 and PATMOS-x on an interannual scale. Seasonally, CCSM3 shows far more trends with high correlation in low cloud fraction and LTS than CM2 as expected. However, the seasonal trends in the observation data do not agree with previous studies. Therefore, based on this study a definitive conclusion cannot be made.

c. Conclusions and Future Work

The low cloud fraction-LTS relationship initially presented by KH93 is not well represented in this study. Two seasons do show the relationship as being significant (pre-

2000 OND and post-2000 JFM). However, the entire season of JAS does have the same relationship presented in KH93 but it is not significant. This is not consistent with KH93 or other more recent studies (Jensen, et al. 2008, Ghate et al. 2009, Zhang et al. 2010). One main reason for this discrepancy could be spatial averaging over the entire study domain. However, this is the method used in KH93 (seasonally averaging over all years over the study domain). The domain in their study is half the size of the one used in this study. Perhaps the larger domain incorporates a wider range of processes that mask the previously identified relationships. Studies with larger domains (Jensen et al. 2008, Ghate et al. 2009, Zhang et al. 2010) averaged by grid box seem to capture the low cloud fraction-LTS relationship. Interestingly, even with a larger domain, the low cloud fraction-LTS relationship in JAS was present. This could mean that large scale processes may not mask the relationship in this season which would be worth studying.

The interannual low cloud fraction in this study was very similar in pattern and percent to KH93, despite the larger domain (Figure 2). This figure shows two climatologies of low cloud fraction and essentially represents interannual low cloud fraction from 1951-2009 from observational data. This is a very interesting representation and merits further analysis. The figure shows a decrease in maximum low cloud fraction from ~72% in KH93 to ~62% in PATMOS-x. This is likely due to the larger domain for this study than that of KH93 and thus, potentially less cloudy areas could be affecting the results especially since more recent studies have shown higher low cloud amounts in this region post-2000 (~80%) (Ghate et al. 2009, Zhang at al. 2010). Still the shifts in magnitude and seasonality are interesting to consider.

It is somewhat reasonable to assume that low cloud fraction has minimally changed on an interannual scale over the past 58 years for this particular region. However, something is happening to LTS in this study. This could easily be a result in the way LTS is calculated (monthly means for each year are calculated and then these are averaged seasonally to get one value per year). This could also suggest that something is different in a long time scale versus short five to six year time scales that have recently been studied. It would be fruitful to obtain LTS observations from other analysis groups to determine if LTS is expected to change over a long time scale in the future. This would have a large effect on GCM low cloud simulations like CCSM3.

Zhang et al. (2010) propose modifying LTS to incorporate lifting condensation level (LCL) and temperature advection. They conclude that a high LCL pressure which corresponds to moist air and cold air advection lead to higher, low cloud fractions and vice versa. Their study indeed shows a much better correlation between low cloud fraction and LTS if that version of LTS is incorporated into a cloud parameterization scheme for years 2000-2006. If LTS requires a change to maintain the same pattern as low cloud fraction post-2000 when previously in KH93, LTS correlated very well with low cloud fraction; does that mean the low cloud fraction-LTS relationship is changing? A better question is *has* this relationship changed since KH93 which looked at years 1951-1981? If so, is this change attributed to better observation methods with the increase in satellite data, a better understanding of MBL clouds in general, or even something like anthropogenic climate change with respect to sea surface temperature increase? These are all questions that barely scratch the surface of possibilities of more in depth analyses using long-term observational datasets like PATMOS-x as they become available.

Overall, it is believed that the domain averaging constraint in this study has lead to different observational results in the low cloud fraction-LTS relationship defined by KH93. While both models appear to represent the relationship, it cannot be determined whether they are accurate as observational results are not conclusive. Future work requires studying the domain by averaging per grid box in order to have a better understanding of spatial variations in low cloud fraction and LTS.

V. References

Anderson, J. L. and the GFDL Global Atmospheric Model Development Team, 2004: The New GFDL Global Atmosphere and Land Model AM2 – LM2: Evaluations with Prescribed SST Simulations. *J. of Climate*, **17**, 4641 – 4673.

Bony, S., and J.-L. Dufresne, 2005: Marine boundary layer clouds at the heart of tropical cloud
feedback uncertainties in climate models. *Geophys. Res. Lett*., **32**, L20806.

CESM, cited 2010: Community Earth System Model 20C3M Experiments. [Available online at http://www.cesm.ucar.edu/working_groups/Change/CCSM3_IPCC_AR4/20C3M.html]

CIMSS-A, cited 2010: PATMOS-x Overview Page. [Available online at http://cimss.ssec.wisc.edu/patmosx/overview.html]

CIMSS-B, cited 2010: PATMOS-x Index Page. [Available online at http://cimss.ssec.wisc.edu/patmosx/doc/level2b_data_description.html]

Collins, W. D., 2001: Parameterized Cloud Overlap for Radiative Calculations in General Circulation Models. *J. Atm. Sci.*, **58**, 3224 – 3242.

___, P. J. Rasch, B. A. Boville, J. J. Hack, J. R. McCaa, D. L. Williamson, J. T. Kiehl, B. Briegleb, C. Bitz, S.-J. Lin, M. Zhang, and Y. Dai, 2004: Description of the NCAR Community Atmosphere Model (CAM3). Tech. Rep. NCAR/TN-464+STR, National Center for Atmospheric Research, Boulder, CO, 226 pp.

___, C. M. Bitz, M. L. Blackmon, G. B. Bonan, C. S. Bretherton, J. A. Carton, P. Chang, S. C. Doney, J. J. Hack, T. B. Henderson, J. T. Kiehl, W. G. Large, D. S. McKenna, B. D. Santer, and R. D. Smith, 2006a: The Community Climate System Model Version 3 (CCSM3). *J. Climate*, **19**, 2122 – 2143.

___, P. J. Rasch, B. A. Boville, J. J. Hack, J. R. McCaa, D. L. Williamson, and B. P. Briegleb, 2006b: The Formulation and Atmospheric Simulation of the Community Atmosphere Model Version 3 (CAM3). *J. Climate*, **19**, 2144 – 2161.

Delworth, T. L. and collaborators, 2006: GFDL's CM2 Global Coupled Climate Models. Part I: Formulation and Simulation Characteristics. *J. of Climate*, **19**, 643 – 674.

Ghate, V. P., B. A. Albrecht, C. W. Fairall, and R. A. Weller, 2009: Climatology of Surface Meteorology, Surface Fluxes, Cloud Fraction, and Radiative Forcing over the Southeast Pacific from Buoy Observations. *J. Climate*, **22**, 5527 – 5540.

Gutman, G. G., 1999: On the monitoring of land surface temperatures with the NOAA/AVHRR: rmoving the effect of satellite orbit drift. *Int. J. Remote Sens.,* **20**, 3407 – 3413.

Heidinger, A. K., and M. J. Pavolonis, 2009: Gazing at Cirrus Clouds for 25 Years through a Split Window. Part I: Methodology. *J. Appl. Meteor. Climatol.*, **48**, 1100-1116.

Hogan, R. J., and A. J. Illingworth, 2000: Deriving cloud overlap statistics from radar. *Q. J. R. Meteorol. Soc.*, **126**, 2903 – 2909.

IPCC-AR4, cited 2010: IPCC Fourth Assesment Report: Climate Change 2007, 3.1 Emissions Scenarios. [Available online at http://www.ipcc.ch/publications_and_data/ar4/syr/en/mains3.html]

Jensen, M. P., A. M. Vogelmann, W. D. Collins, G. J. Zhang, and E. P. Luke, 2008: Investigation of regional and seasonal variations in marine boundary layer cloud properties from MODIS observations. *J. Climate*, **21**, 4955-4973.

Kalnay et al., 1996: The NCEP/NCAR 40-year reanalysis project. *Bull. Amer. Meteor. Soc*., **77**, 437-470.

Klein, S. A., and D. L. Hartmann, 1993: The seasonal cycle of low stratiform clouds. *J. Climate*,
6, 1587-1606.

Manning, M. R., J. Edmonds, S. Emori, A. Grubler, K. Hibbard, F. Joos, M. Kainuma, R. F. Keeling, T. Kram, A. C. Manning, M. Meinshausen, R. Moss, N. Nakicenovic, K. Riahi, S. K. Rose, S. Smith, R. Swart, and D. P. van Vuuren, 2010: Misrepresentation of the IPCC CO_2 emission scenarios. *Nature Geoscience*, **3**, 376 – 377.

NOAASIS, cited 2010: NOAA Satellite and Information Service-AVHRR. [Available online at http://noaasis.noaa.gov/NOAASIS/ml/avhrr.html]

Pavolonis, M. J. and A. K. Heidinger, 2004: Daytime Cloud Overlap Detection from AVHRR and VIIRS. *J. App. Meteor.,* **43**, 762 – 778.

___, A. K. Heidinger, and T. Uttal, 2005: Daytime Global Cloud Typing from AVHRR and VIIRS: Algorithm Description, Validation, and Comparisons. *J. App. Meteor.*, **44**, 804 – 826.

Petty, G. W., 2006: A First Course in Atmospheric Radiation. 2nd ed. Sundog Publishing, 147,
459 pp.

Rausch, J., A. Heidinger, and R. Bennartz, 2010: Regional assessment of marine boundary layer cloud microphysical properties using the PATMOS-x dataset. *Submitted to J. Geophysical Research August 2010.*

Rotstayn, L. D., 1997: A physically based scheme for the treatment of stratiform clouds and precipitation in large-scale models. I: Description and evaluation of the microphysical processes. *Q. J. R. Meteorol. Soc.*, **123**, 1227 – 1282.

Salby, M. L., 1996: Fundamentals of Atmospheric Physics. Academic Press, Inc., 71, 627 pp.

Smith, R. N. B., 1990: A scheme for predicting layer clouds and their water content in a general circulation model. *Q. J. R. Meteorol. Soc.*, **116**, 435 – 460.

Stephens, G. L., 2004: Cloud feedbacks in the climate system: A critical review. *J. Climate*, **18**,
237-273.

Stowe, L. L., H. J. Jacobowitz, G. Ohring, K. R. Knapp, and N. R. Nalli, 2002: The Advanced
Very High Resolution Radiometer (AVHRR) Pathfinder Atmosphere (PATMOS)
Climate Dataset: Initial Analyses and Evaluations. *J. Climate,* **15**, 1243-1260.

Tiedtke, M., 1993: Representation of Clouds in Large-Scale Models. *Mon. Weather Rev.*, **121**, 3040 – 3061.

Wittenberg, A. T., A. Rosati, N.-C. Lau, and J. J. Ploshay, 2006: GFDL's CM2 Global Coupled Climate Models. Part III: Tropical Pacific Climate and ENSO. *J. Climate*, **19**, 698 – 722.

Wood, R. and D. L. Hartmann, 2006: Spatial Variability of Liquid Water Path in Marine Low Cloud: The Importance of Mesoscale Cellular Convection. *J. Climate*, **19**, 1748 – 1764.

Zhang, G., A. M. Vogelmann, M. P. Jensen, W. D. Collins, and E. P. Luke, 2010: Relating Satellite-Observed Cloud Properties from MODIS to Meteorological Conditions for Marine Boundary Layer Clouds. *J. Climate*, **23**, 1374 – 1391.